
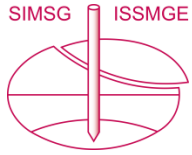




# Invited Lecture Papers

**Proceedings of the XVI ECSMGE**
**Geotechnical Engineering for Infrastructure and Development**
ISBN 978-0-7277-6067-8


doi:10.1680/ecsmge.60678

# Ground improvement versus hybrid foundation and deep foundation: three case histories of European significance

## Amélioration du sol contre fondation hybride et fondation profonde: trois cas d'importance européenne

D. Adam[*1]

[1] *Institute of Geotechnics, Vienna University of Technology, Vienna, Austria*
** Corresponding Author*

ABSTRACT The focus of this invited paper is on the comparison of different foundation concepts for three case histories of European significance. The stadium in the Austrian city of Klagenfurt was designed and built for EURO 2008 (Austria and Switzerland) in slightly consolidated soft lacustrine clays. The shallow foundation rests on floating stone columns installed using the vibro replacement technique allowing controlled, large, time-dependent settlements. For the Combined Cycle Power Plant Malženice near Bohunice (Slovakia) a hybrid foundation concept was executed in collapsible aeolian silt deposits (loess). The ground was initially improved by the vibro replacement technique and the final cementation of the stone columns produced deep foundation elements. The new spectacular cable-stayed bridge over the Sava River is the new landmark of Belgrade (Serbia). The 200 m tall pylon of the 965 m long bridge rests on a closed box foundation made of a clasping diaphragm wall with large-diameter bored piles inside. Thus, the highly concentrated loads are transferred into the over-consolidated marls at depth. The different foundation concepts are compared and discussed. It is illustrated that all the concepts are justified considering the ground conditions, structural and serviceability requirements of the buildings, and economical factors (time and cost).

RÉSUMÉ L'objectif de cet article est de comparer trois concepts de fondations pour d'importants projets européens. Le stade de la ville autrichienne de Klagenfurt a été conçu et construit sur des argiles molles légèrement consolidées pour l'EURO 2008 (Autriche et Suisse). La fondation superficielle repose sur des colonnes ballastées flottantes installées avec la technique de vibro remplacement permettant le contrôle des tassements avec le temps. Pour la centrale à cycle combiné de Malženice près de Bohunice (Slovaquie) un concept de fondation hybride a été exécuté dans des dépôts de limon éoliens sensibles (loess). Le sol a été initialement amélioré par la technique de vibro remplacement et la cimentation finale des colonnes ballastées a produit des éléments de fondation profonde. Le nouveau spectaculaire pont à haubans sur la rivière Sava est le nouveau point de repère de Belgrade (Serbie). Le pylône de 200 m de haut du long pont de 965 m de longueur repose sur une "boîte" fermée composée de voiles blindés et des pieux forés de grand diamètre. Ainsi, les charges fortement concentrées sont transférées directement dans les profondes marnes sur- consolidées. Les différents concepts de base sont comparés et discutés. Il est illustré que tous les concepts sont justifiés compte tenu des conditions du sol, exigences structurelles et de fonctionnement des bâtiments, et les facteurs économiques (temps et coût).

## 1 EURO 2008 STADIUM KLAGENFURT (AUSTRIA) GROUND IMPROVEMENT CONCEPT

### *1.1 Introduction*

In 2008 the European Soccer Championship took place in Austria and Switzerland. Klagenfurt was one of the venues. The new so called Wörthersee Stadium was situated near the centre of Klagenfurt close to the Wörthersee, a large glacial lake in Carinthia.

The project consists of the stadium oval with the integrated west building and three (temporary) canopied grandstands for 31,000 spectators. A new soccer academy building and a multifunctional gymnasium are directly connected to the oval. The stadium was designed in such a way that the upper stands of the three grandstands can be demolished. The characteristic shape remains but load is considerably reduced.

Originally a bored pile foundation was designed for the west building due to the unfavourable ground

conditions. An alternative shallow floating raft foundation on stone columns using the vibro replacement technique was actually installed. For the foundation of the girder and column structures of the three grandstands, the soccer academy building and the multifunctional gymnasium, as well as the ground beneath the highly loaded sections of the access ramp on the south west side of the stadium the ground was improved by stone columns. Due to the unfavourable ground conditions settlements of the order of a maximum of 20 cm were predicted so that the deformation compatibility of the particular structures had to be carefully taken into consideration.

**Figure 1.** EURO 2008 Stadium Klagenfurt.

## 1.2 *Ground conditions*

Prior to construction ground exploration and soil investigation was performed in two phases. Rotational core drillings and heavy dynamic probing (DPH) and moreover, seismic investigations to determine the interface between soft soil and bed rock revealed the following soil structure on the site of the stadium (Ingenieurgemeinschaft Garber & Dalmatiner Zivilingenieure 2005a,b and Bautechnische Versuchs- und Forschungsanstalt Salzburg 2006):

Beneath the topsoil young unconsolidated sediments consisting of medium to coarse (gravelly) sands and silt (loam) are deposited up to a depth of 10 to 12 m below surface. Loose to medium dense sands predominate with increasing depth. These layers are underlain by young unconsolidated lake deposits consisting of medium dense silty fine sands followed by silty and clayey lake deposits up to 30 to 48 m beneath surface. Horizontally layered (very) soft clayey silts predominate and alternate with thin layers of silty fine sands and fine sandy silts. These lake deposits rest on sands and the ground moraine, the depth of the underlying bed rock consisting of sound quartz phyllite varies in a wide range below surface from about 31 m in the north to about 60 m in the south.

The groundwater table was found in the drillings at an average depth of about 2.3 m. The groundwater level fluctuates seasonally in a range of about 2.5 m on average. The groundwater is near the surface, thus influencing the soil conditions significantly.

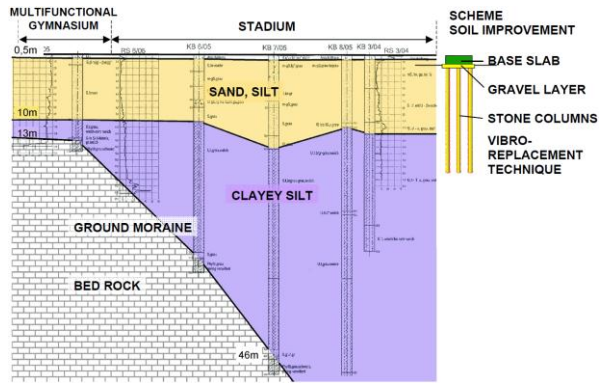


**Figure 2.** Ground conditions at the site of the stadium (schematic).

## 1.3 *Ground improvement and foundation concept*

Beneath all structures (west building, girder and column structures of the three grandstands, the soccer academy building and the multifunctional gymnasium, various single foundations) the ground was improved by installing stone columns and was thus prepared for the shallow foundations. The stone columns have a length of about 10 to 18 m below the surface

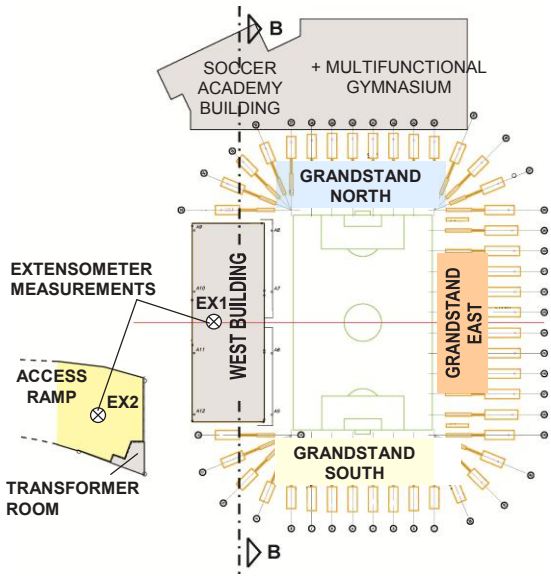


**Figure 3.** Layout of foundation scheme of several structures of the stadium.

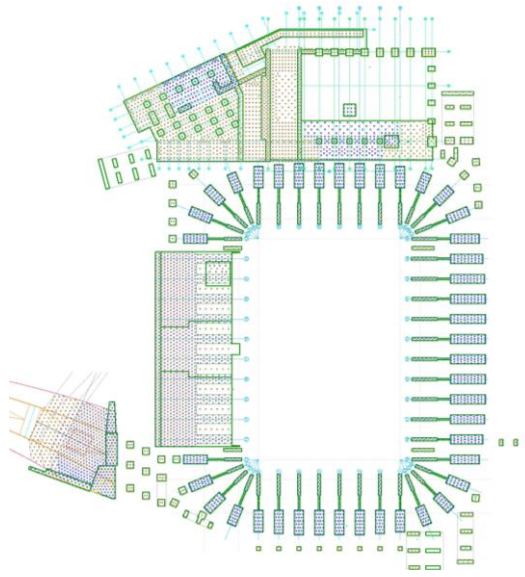

**Figure 4.** Layout of executed stone columns.

and were arranged taking into account the calculated foundation pressures and the soil interfaces found during installation. Thus, it was intended to homogenize the ground conditions on the one hand and to minimize the settlements and differential settlements on the other. Moreover, it was intended to accelerate the consolidation process in the ground through the highly permeable stone columns (Adam & Geotechnik Adam ZT GmbH. 2008c).

In addition the liquefaction potential of the collapsible soil in the upper layers was reduced to increase the resistance of the soil to seismic activity in case of an earthquake. This was achieved by improving the shear parameters and increasing the overall permeability of the ground. Moreover, the compactable soil was improved around the stone columns by the vibratory installation process using the bottom feed vibrator technique. For drainage and load distribution a gravel layer was placed as fill above the improved ground with thickness varying according to the needs of the structure.

The reinforced concrete slab of the west building was extended by a cantilever comprising a length of about 2 m in order to improve the pressure distribution due to the non-uniform loads beneath the raft foundation. Additionally, at the rear of the west building a preloading was applied to anticipate a specific portion of the expected settlements. Settlement measurements revealed that up to about 12 cm of settlements occurred from preloading the fill. Differential settlements between the west building and the adjacent (temporary) grandstands were taken into account by superelevating the raft foundation of the west building.

In the area of the outer stairs in the northwest the soil had been preloaded by a demolished building. The maximum allowable soil pressure was limited to 115 kN/m² since no deep ground improvement could be performed there. Soil was replaced with recycled concrete aggregate to a thickness of 100 cm.

In the lower part of the access ramp in the southwest of the oval the ground was not improved. The 10.5 m high ramp adjacent to the west building was filled on ground improved by stone columns for the following reasons:

- Reduction of settlements to minimize deformations which could affect the west building.
- Acceleration of settlements by increasing the overall permeability of the ground to reduce the residual consolidation settlements to a minimum for the incorporated concrete structures, such as

the transformer room, retaining walls and the bridge structure.
- Increase of shear strength of the soil to avoid local ground failure due to quick filling procedure.
- Providing sufficient safety against mechanical ground failure of structures which are incorporated into the ramp (especially the transformer room and the retaining structures).

Preloading of the area in front of the ramp anticipated a considerable portion of predicted settlements. The preloading fill was removed after defined settlements occurred and the concrete structures were constructed. In defined areas of the multifunctional gymnasium with lower loads (playing field, access area) soil was replaced instead of stone columns being placed. The base slab of the gymnasium was filled with concrete at the latest date after completion of the structure to minimize differential settlements between the structure and the base slab.

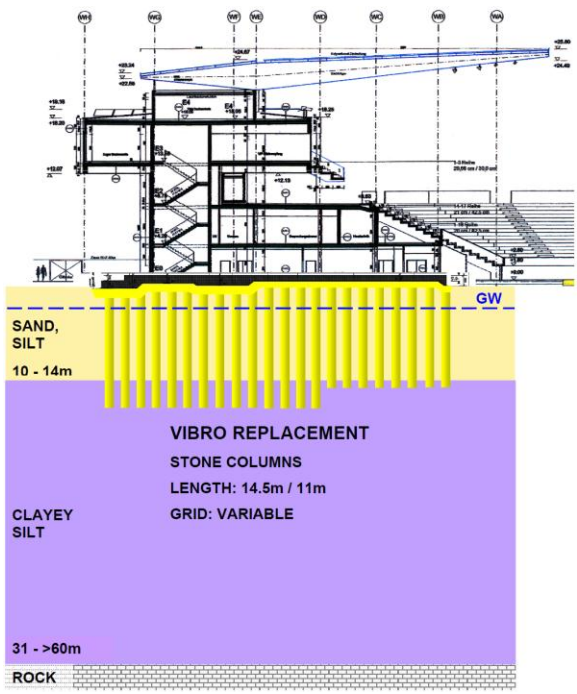


**Figure 5.** Cross section of the west building, raft foundation and stone columns.

Ground improvement was checked by following test procedures:

- Heavy dynamic probing (DPH) before and after installation of stone columns to verify the improved properties of the ground.
- Dynamic load plate tests with the Light Falling Weight Device (LFWD) to check the bearing capacity and stiffness of the gravel fill layers and the exchanged soil layers.
- Roller integrated Continuous Compaction Control (CCC) with vibratory rollers to check all fill layers and the formation layers of the foundations (e.g. raft foundation).

### *1.4 Prediction of settlement behaviour*

The deep soil improvement with installed stone columns caused an increase of the bearing capacity of the ground, compaction of the soil by activating the self-compaction potential of the soil, a homogenization of the ground properties and an acceleration of consolidation settlements by increasing the overall permeability. Below the stone columns lake deposits comprise relatively homogeneous conditions but long-term settlements of about 3 to 6 cm after completion were predicted by the consolidation process and possibly by a creeping process as well. Due to the permeability and the stiffness of the soil it was assumed that he consolidation process will take some years.

In the design phase of the foundation concept settlement calculations were performed in order to predict the settlements and differential settlements for each building. In Table 1 the total settlements including the consolidation process are presented.

**Table 1**: Predicted settlements (expected values) for the west building taking into consideration soil improvement with stone columns and an extended slab (Adam & Geotechnik Adam ZT GmbH. 2008c).

| Location | s | Δs | length | inclination | |
|---|---|---|---|---|---|
| | [mm] | [mm] | [m] | [%] | [-] |
| corner SW | 150 | - | - | - | - |
| corner NW | 130 | - | - | - | - |
| corner NE | 80 | - | - | - | - |
| corner SE | 90 | - | - | - | - |
| outer side W | - | 20 | 101 | 0.02 | 1/5050 |
| side N | - | 50 | 34 | 0.15 | 1/680 |
| inner side E | - | 10 | 101 | 0.01 | <1/10000 |
| side S | - | 60 | 34 | 0.18 | 1/567 |

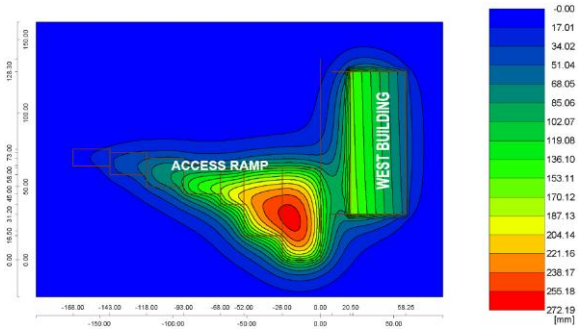


**Figure 6.** Calculated total settlements and determination of the mutual influence of west building and access ramp.

Settlement calculations revealed that settlements along the outer side in the west of the west building would be be significantly larger compared to the inner side in the east because of the non-uniform load distribution. Moreover, the calculation results showed that the settlements in the north would be smaller than in the south of the west building. On the one hand the rock bed is not so deep below surface in the north than in the south and on the other hand the settlements of the access ramp affected the southern part of the west building as well. For these reasons an additional preloading fill was installed in the south of the west building.

The differential settlements within the west building were estimated to about 9 cm, nevertheless the derived angular rotation of the west building was within the limits. Thus, by means of the large dimensions the serviceability of the building was not affected by the differential settlements.

### *1.5 Monitoring of settlements*

Settlement monitoring during the various construction sequences was performed in order to provide continuous observations of the settlements of the ground. Measurement points for long-term settlement monitoring have been installed at the west building, the girder and column structures of the three grandstands, and the transformer building.

At the west building in 2010 the settlements amounted up to a maximum of 14 cm at the outer side (east) and up to maximum 7 cm (west).

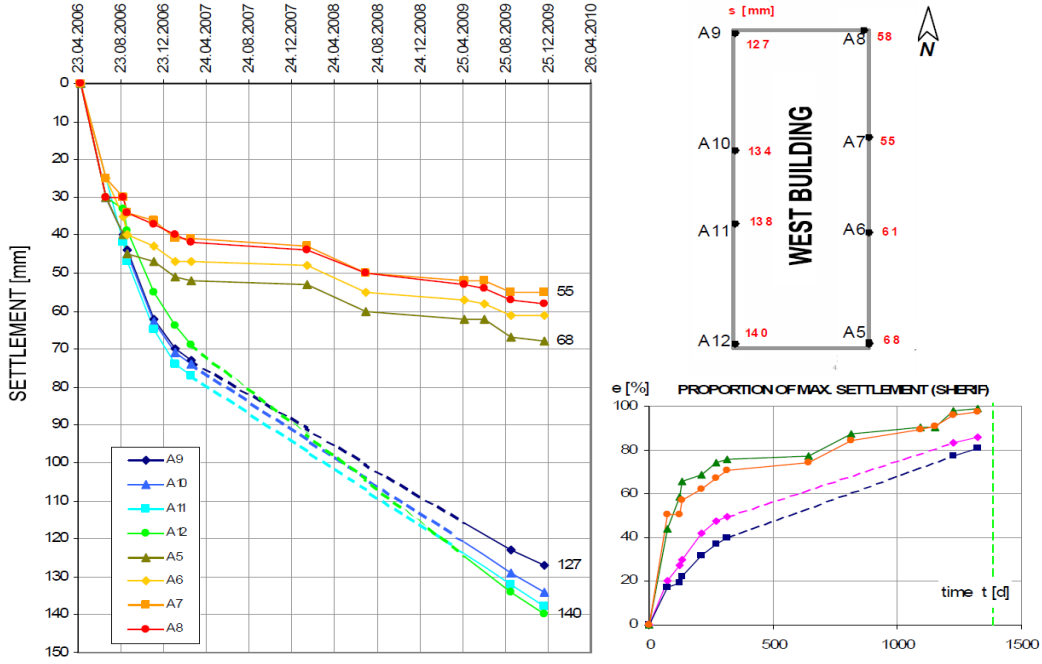


**Figure 7.** Geodetic settlement measurements for the west building, position of the measurement points and prediction of final settlements according to Sherif; measurement campaign until December 2009.

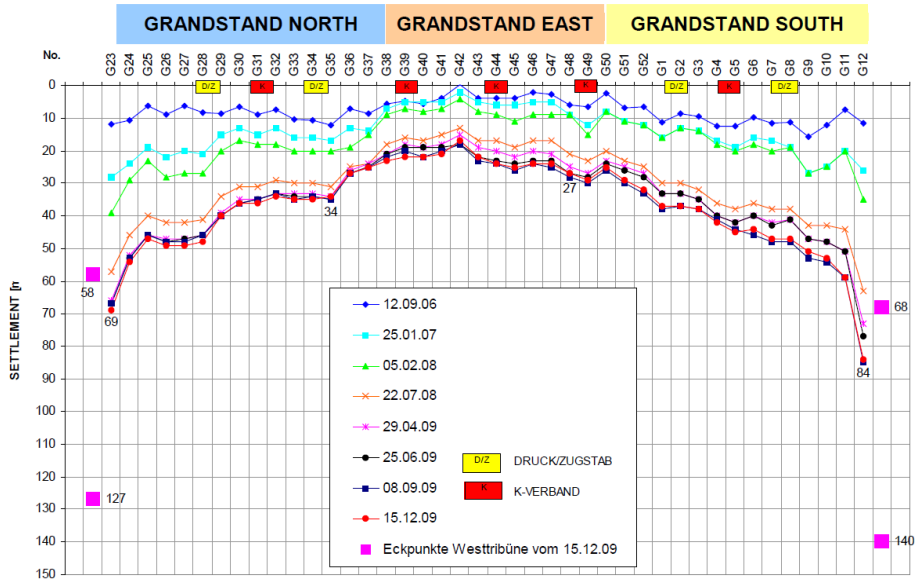


**Figure 8.** Settlements over time at the girder and column structures of the three grandstands.

In comparison to the settlement measurements before a remarkable increase of the settlements was observed in the south western corner of the stadium.

Analyses of the progress of settlements over time revealed that the outer and the inner sides of the west building settled unequally. In the period from March 2007 to December 2009 (about 33 months) the inner side settled by about 1.5 cm while the outer side settled by about 7 cm. Moreover, the south western corner (about 7 cm) is affected more by the ramp than the north western corner (about 5.5 cm). As expected the settlements are influenced by the superposition of the deformations of the west building and the ramp.

Progress of settlements over time and the evaluation according to Sherif (ÖNORM B 4431-2) show that the settlements decay already at the inner side but until now not at the outer side. According to the evaluation according to Sherif about 80% of the total settlements occurred until 2010 so that about 20% are still to be expected in the future.

In spite of the differential settlements between the outer and the inner side of the west building the maximum gradient of the VIP box in the upper floor is in of the order of about 0.2% according to measurements. Thus, the serviceability of the building is not affected by the differential settlements. The differential settlements at the girder and column structures of the three grandstands are in a range from 0 to 0.8 cm. Only between the structures G11 and G12 and between G23 and G24 adjacent to the west building the differential settlements are larger as expected due to the influence of the west building.

However, different deformations can be taken into account by readjusting the tension rods of the bracings. Differential settlements are limited to 2 cm only at the foundations of the girder and column structures with fixed bracings consisting of tension and pressure rods (so called K bracings). However, actual measured values are far below this limiting value.

Settlement measurements show that total settlements have only marginally increased. However, it is expected that certain additional consolidation settlements will occur.

Measured total settlements at the ramp show maximum values of about 18 cm. By means of the influence of the west building additional settlements occur at measurement point SP34. Additional settlements at measurement point SP36 are caused by the loads on all sides and the extensive settlement influence of the access ramp. The prediction of the final settlements according to Sherif has revealed that about 80% of the total settlements have occurred up to the end of year 2010.

In a large scale well instrumented field trial consisting of multilevel-piezometers, multilevel-extensometers and earth pressure cells as well as a horizontal inclinometer the performance of the floating stone column foundation was investigated. The measurements give valuable insight into the installation process of stone columns and the evolution of pore water pressures and settlements over time beneath the 10.5 m high access ramp (Gäb et al. 2007).

In Figure 11 results of extensometer and multilevel-piezometer measurements are presented revealing the effect of increasing the over-all permeability in the zone of the stone columns. Pore water pressures decrease rapidly after completion of stone column installation thus accelerating consolidation settlements in the ground. Below the stone columns the permeability of the ground is low so that the decrease of pore water pressure and consolidation settlements take a long time, presumably some years.

### *1.6 Back analysis of settlements of the west building*

A series of finite element analyses have been performed for this project and comparison of field measurements with 2D analyses employing different constitutive models has been presented in (Gäb et al. 2008) for the heavily instrumented trial field set up in the area of the ramp. Thus, these results will not be repeated here but results from back analysis of the settlement behaviour of the west building will be discussed in the following (Adam et al. 2010). In addition to the settlement measurements shown in Figure 9 an extensometer has been installed at the west building (location see Figure 3) and these measurements will be considered, too.

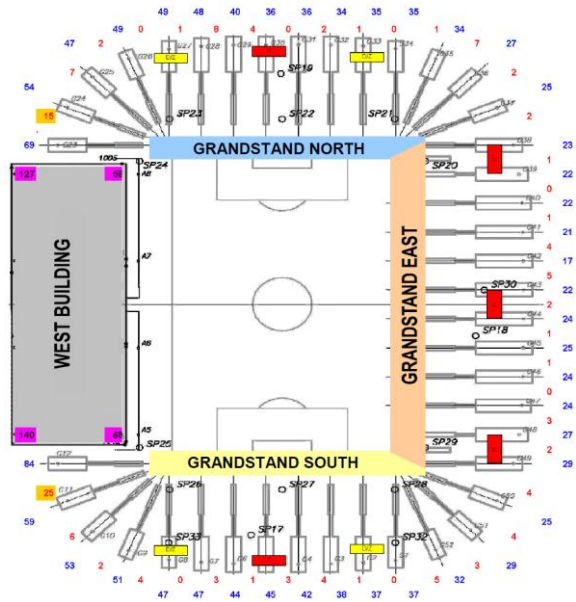


**Figure 9.** Geodetic settlement measurements (blue; unit: mm) and differential settlements (red; unit: mm) between the girder and column structures of the three grandstands; measurement campaign of December 2009.

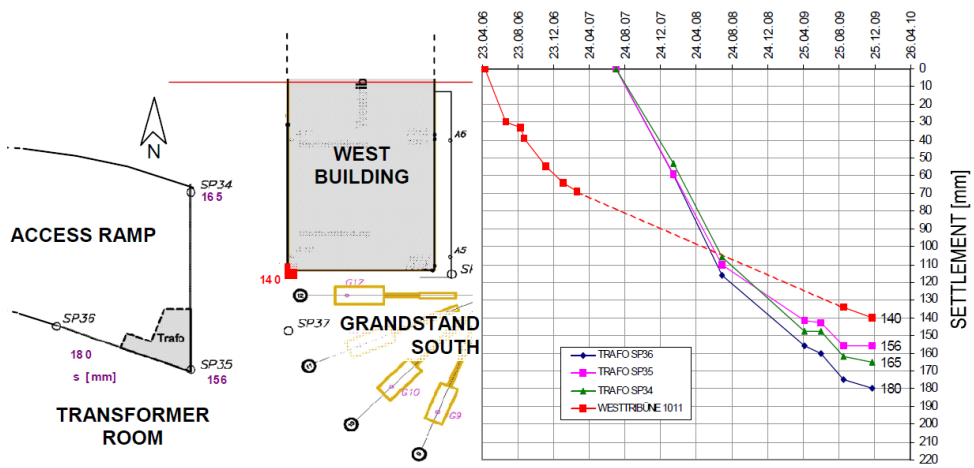


**Figure 10.** Geodetic settlement measurements at transformer room (SP 35) and access ramp (SP 34, SP 36) compared to the south-western corner of the west building (red); measurement campaign until December 2009.

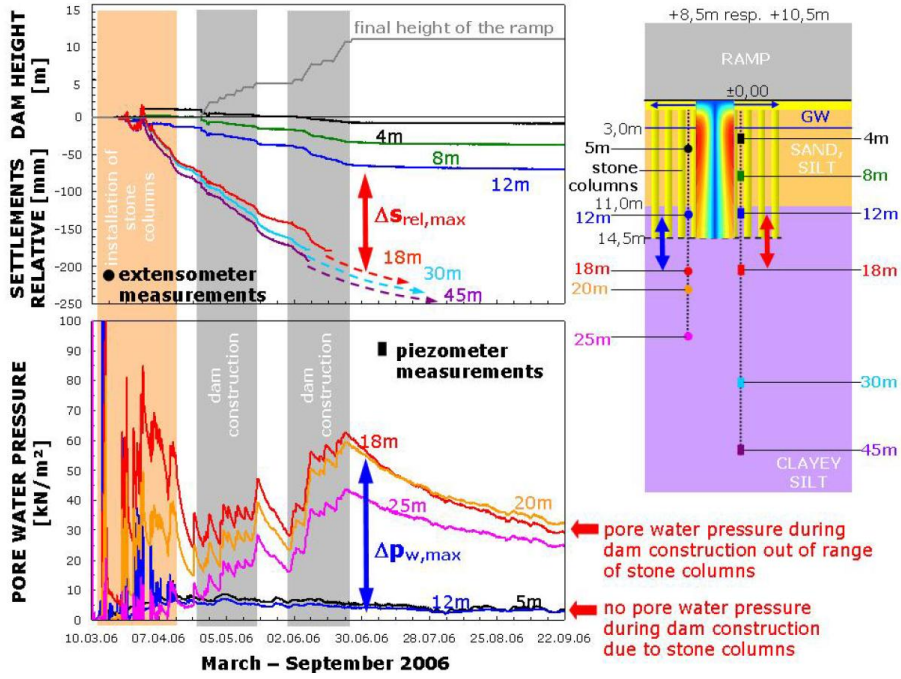


**Figure 11.** Results of the large scale field trial to investigate the performance of the floating stone columns foundation beneath the access ramp (Gäb et al. 2007).

### *1.6.1 Short description of numerical and constitutive models*

Considering the ground conditions a 3D model would be required to capture the inclined layers of soil in detail. However, for this preliminary study a cross section through the middle of the west building was taken postulating plane strain conditions (see Figure 12). The stone columns were modelled as "walls" with depths of 14.5 m on the left side and 10.5 m on the right side respectively. The space between the stone columns is 0.9 m. Figure 12 also shows the different soil layers according to Figure 2. It is noted that for simplicity the layers were assumed as horizontal. The rock (quartz phyllite) was not modelled, because its influence on the settlement behaviour could be considered negligible. Around the stone columns a zone was introduced in which the material properties have been adjusted. In this sand layer ("Sand dense") the stiffness has been increased due to significant compaction of the originally loose sand during the installation of the columns. The Soft Soil Creep model (SSC) was used for this study which

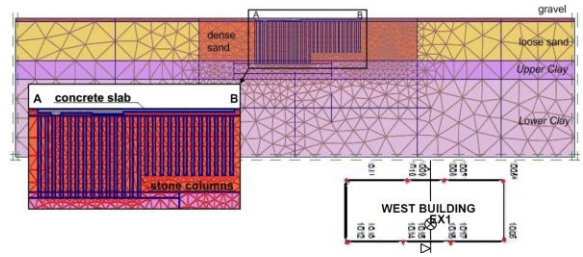


**Figure 12.** Cross section and 2D numerical model.

is an extension of the so-called Soft Soil model, both available in model library of the finite element code Plaxis (Brinkgreve et al. 2006). The Soft Soil Creep model is based on the approach proposed by Bjerrum (1967) and Janbu (1967) and considers time and strain rate effects. Thus, the total strain consists of a time independent elastic part and a time dependent visco-plastic part. The creep effects are introduced by the modified creep index $\mu^*$, which is related to the creep index $C_\alpha$. The constitutive parameters required for the SSC model are the modified compression index $\lambda^*$, the modified swelling index $\kappa^*$, the modified

**Table 2:** Material parameters for soil layers.

| | $k_x$ | $k_y$ | $\gamma$ | $\gamma$ | c | $\varphi$ | $\Psi$ | $\nu$ | $\kappa^*$ | $\lambda^*$ | $\mu^*$ | | OCR | $K_{0,nc}$ |
|---|---|---|---|---|---|---|---|---|---|---|---|---|---|---|
| | [m/s] | [m/s] | [kN/m³] | [kN/m³] | [kN/m²] | [°] | [°] | [-] | [-] | [-] | [-] | | [-] | [-] |
| *Upper Clay* | 2.6E-9 | 7.9E-9 | 16 | 19 | 10 | 22.5 | 0 | 0.2 | 0.0053 | 0.028 | 0.0009 | | 1.3 | 0.617 |
| *Lower Clay* | 2.4E-8 | 2.3E-7 | 16 | 19 | 10 | 22.5 | 0 | 0.2 | 0.005 | 0.026 | 0.00085 | | 1.3 | 0.617 |
| | $k_x$ | $k_y$ | $\gamma$ | $\gamma$ | c | $\varphi$ | $\Psi$ | $\nu$ | $E_{50}^{ref}$ | $E_{oed}^{ref}$ | $E_{ur}^{ref}$ | m | OCR | $K_{0,nc}$ |
| | [m/s] | [m/s] | [kN/m³] | [kN/m³] | [kN/m²] | [°] | [°] | [-] | [MN/m²] | [MN/m²] | [MN/m²] | [-] | [-] | [-] |
| *Loose sand* | 1E-5 | 1E-5 | 18 | 21 | 0.1 | 27.5 | 2 | 0.2 | 16 | 16 | 80 | 0.55 | 1 | 0.538 |
| *Dense sand* | 1E-5 | 1E-5 | 18 | 21 | 0.1 | 27.5 | 2 | 0.2 | 40 | 40 | 120 | 0.65 | 1 | 0.538 |
| *Stone columns* | 1E-5 | 1E-5 | 20 | 23.5 | 0.1 | 35 | 5 | 0.2 | 250 | 25 | 75 | 0.3 | 1 | 0.426 |
| *Gravel* | 1E-5 | 1E-5 | 20 | 20 | 0.1 | 35 | 0 | | 35 | 35 | 105 | 0.5 | 1 | 0.426 |
| *Concrete slab* | - | - | 25 | - | - | - | - | 0.2 | 3E7 | - | - | - | 1 | - |

creep index $\mu^*$, the friction angle $\varphi'$, cohesion c', dilatancy angle $\psi$, Possions's ratio $\nu$ and coefficient of earth pressure at rest $K_{0,}^{nc}$. These parameters can be determined by standard triaxial and oedometer tests. A detailed description of the model can be found in (Vermeer and Neher 2000). The Soft Soil Creep model was used for the clayey silt layers, for all other soil layers and the stone columns the Plaxis Hardening Soil model (Brinkgreve et al. 2006) was used. The parameters are summarized in Table 2.

### *1.6.2 Results of numerical back-analysis*

Results from the numerical back-analysis are compared to the measurements of points (1007/1008 (A10) - 1009/1010 (A11) and 1014/1015 (A6) - 1016/1017 (A7)) according to Figure 13. These data correspond to the simulated vertical displacement of points A and B (Figure 12). Furthermore, available extensometer measurements (EX1) are taken into consideration. The results for vertical displacements versus time are illustrated in Figure 13.

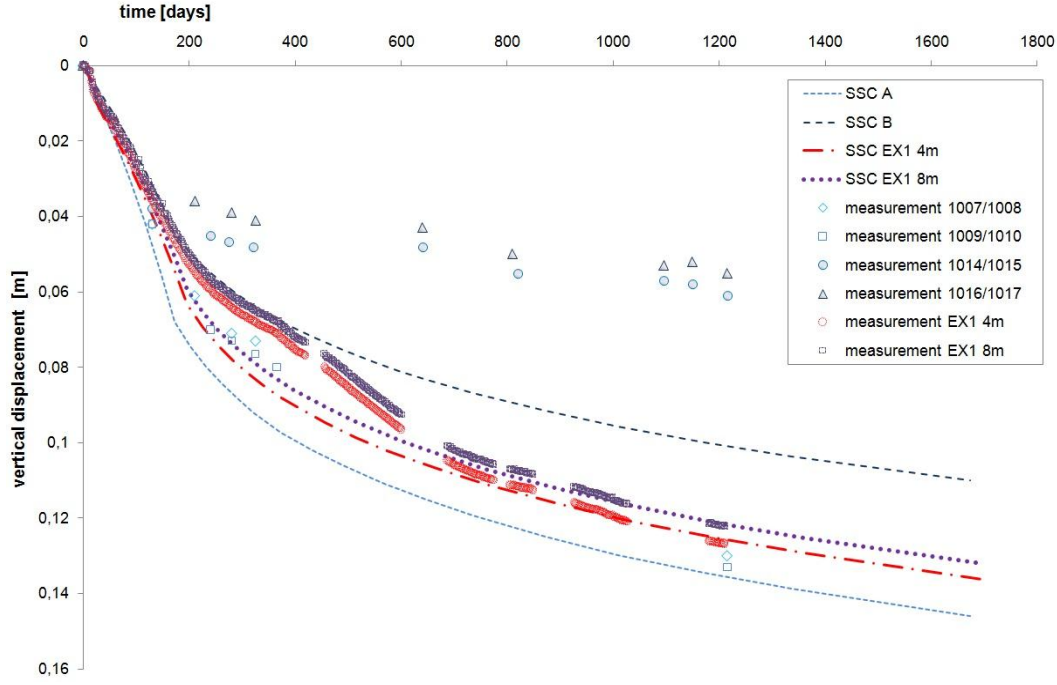


**Figure 13.** Results of back-calculation using SSC model: vertical displacements.

The calculated vertical displacements in point A agree very well with the measurements of 1007/1008 and 1009/1010. Also the measurements obtained form of the extensometer in 4 and 8 m depth can be reproduced very well. However, vertical displacements in point B are too high compared to measured values. The reason for this discrepancy is not yet clear and needs further investigations. It is likely that the load in this section has been overestimated.

## 2 CCPP MALŽENICE (SLOVAKIA) HYBRID GROUND IMPROVEMENT AND DEEP FOUNDATION CONCEPT

### *2.1 Introduction*

E.ON Elektrárne, s.r.o., SPP Kompresorová stanica 3, SK-919 33 Trakovice, the Trakovice based subsidiary of E.ON Kraftwerke GmbH in Hannover, Germany, erected a 400 MW gas fired combined cycle power plant (CCPP) at Malženice, in the western part of Slovakia, roughly 60 km north east of the capital Bratislava. The E.ON Elektrárne s.r.o. plant has been designed as a combined cycle power plant with an efficiency of 58% resulting from the combination of a gas turbine system and a steam turbine system and supplies over 600,000 households with electricity, efficiently and reliably throughout the whole year. The power plant is fuelled by environmentally friendly natural gas. The cooling water is taken from the river Dudvah. Commercial operation of this gas power station started in 2012.

The investor and operator of the Malženice gas and steam turbine power plant is the Trakovice based E.ON Elektrárne s.r.o. SIEMENS AG from Germany was appointed as general contractor. Civil construction works were carried out by the consortium Porr & Alpine Mayreder from Austria. On behalf of the consortium Porr & Alpine Mayreder, the civil design works were done by the Austrian offices Zorn & Nowy ZT GmbH, Heindl & Partner ZT GmbH and Convex ZT GmbH.

The foundation concept developed, based on a detailed investigation of the ground conditions at the site of the planned CCPP, combines stabilization of the soil beneath the base slab of the structures of the planned CCPP (ground improvement) and the vibro replacement technique to produce pile-like bearing elements in the form of stone columns and grouted stone columns and to improve the soil deeply (deep foundation and deep soil improvement). This innovative hybrid foundation concept is presented in the following.


**Figure 14.** Visualisation of the planned gas fired combined cycle power plant (CCPP 400 MW) at Malženice, in the western part of Slovakia, roughly 60 km North East of the capital Bratislava.

### *2.2 Ground conditions*

According to the geomorphologic classification the area belongs to the Danube lowlands region, the Danube plain entity, the subdivision of Trnavskápahorkatina (hilly area) and the part of Trnavská tabula's (tableland). Topography of the area is flat, with gentle depressions which were formed by the local steam patterns. The altitude above sea level varies between about 166 to 168 m a.s.l. (m B.).

From the geological point of view the area at issue is part of the Danube Neogene basin which started to take shape in the Upper Badenian. The older neogeneous series of strata occur at the peripheral parts of the basin in the broader area of interest. The uppermost neogeneous series of strata of Dacian and Rumanian which is widespread in the Trnavská pahorkatina (hilly area) are lying discordantly over the variegated Pontian. Lithological development of the sediments of Dacian and Rumanian is considerably variable. The latter are most frequently represented by gravelly-sandy sediments and by the strata of clays and strongly clayey gravels. The Quaternary is built up of aeolian and fluvial sediments. Aeolian sediments are represented by loess (corresponding to clays of low plasticity), the thickness of which varies

depending on the morphology of the sub-base. The loess was blown in the Pleistocene on the pre-existing hilly surface. They are of light-yellow to light-brown colour, considerably monotonous, with sporadic content of fine sand. They often include the calcareous concretions of size mainly 1-2 cm, sporadically however even larger. Calcium carbonate imparts stability to the loess, which has a characteristic vertical jointing. Among the characteristics of loess is collapsibility. In the deeper horizons the amount of the clayey fraction increases.

Almost the entire area is covered on the surface by the loess which, from the point of view of groundwater occurrence, is significant. Under the loess occurs the gravelly-sandy complex of strata of the Upper Pliocene and Quaternary, probably alluvium of river Váh, which is well water-saturated. It is represented by gravels and sands which frequently alternate, particularly in the horizontal direction. The thickness of the water-saturated complex of strata is several meters.

The gravelly-sandy series of strata forms the vast groundwater reservoir with unconfined as well as confined water level. Groundwater resources of the gravelly-sandy aquifer are recharged by the infiltration of precipitation from the region of Malé Karpaty (Little Carpathian Mts.) and by infiltration from the water sources which are locally cut down into the gravelly-sandy sediments.

The detailed ground conditions at the site of the planned power plant were explored in summer 2008. The results and conclusions of geological investigations carried out in the past in the vicinity of the area of interest were also taken into account. The soil investigations comprised field investigations in the form of exploration pits, core drillings, standard penetration tests in the boreholes (SPT), heavy dynamic probing (DPH), penetration tests (CPT) and cross-hole seismic measurements, and soil mechanics and chemical laboratory tests. The main findings regarding the stratigraphy and soil conditions are concluded in the following.

Agriculture soil, anthropogenic backfills and fills (layer complex A) have been found up to a depth of about 1 m below the ground level of the nearly horizontal site (top between about 167 m and 168 m B.).

Below the anthropogenic backfills and fills are aeolian sediments in the form of loess and loess loams (layer complex B) up to about 14 m to 16 m b.g.l. (Note: m b.g.l. = meter below ground level). Sandy-clayey silt with medium plasticity and lime concretions up to 40 mm prevail in the lower horizon. In the transition zone to the alluvial sediments beneath sandy, stiff to very stiff clay with lime concretions up to 80 mm are found. The loess soil complex can be subdivided on the basis of macroscopic evaluations, laboratory tests and penetration tests into several horizons.

The first loess horizon of aeolian sediments tends to be collapsible and was found across the entire investigation area up to a maximum depth of about 6 m b.g.l. They consist of clay of low plasticity and hard to stiff consistency, and occasionally of loam of low plasticity and hard to stiff consistency.

The second loess horizon was also found across the entire investigation area at depths 3 to 6 m b.g.l. to 9 to 11 m b.g.l. They consist of aeolian sediments represented by clay of low plasticity and hard to stiff consistency, and by loam of low plasticity and hard to, sporadically, stiff consistency.

It is necessary to point out that the aeolian sediments of the first and second loess horizons are collapsible. This property was confirmed by the results of laboratory tests carried out on undisturbed soil samples and indirectly by the low bulk density and high porosity of the loess(loam)s. The loess texture was even disturbed by higher load, i.e. they have collapsed without additional wetting.

Under the loess sediments, but above the gravel layer complex, at depths of about 9 to 10 m b.g.l. through 13 to 18 m b.g.l. were found degraded loesses consisting mainly of clay of low and intermediate plasticity and hard to stiff consistency, and, sporadically, of loam of low plasticity and hard to stiff consistency. Typical for this horizon is the occurrence of $CaCO_3$ nodules and strongly calcareous intercalations, the amount of which increases with depth.

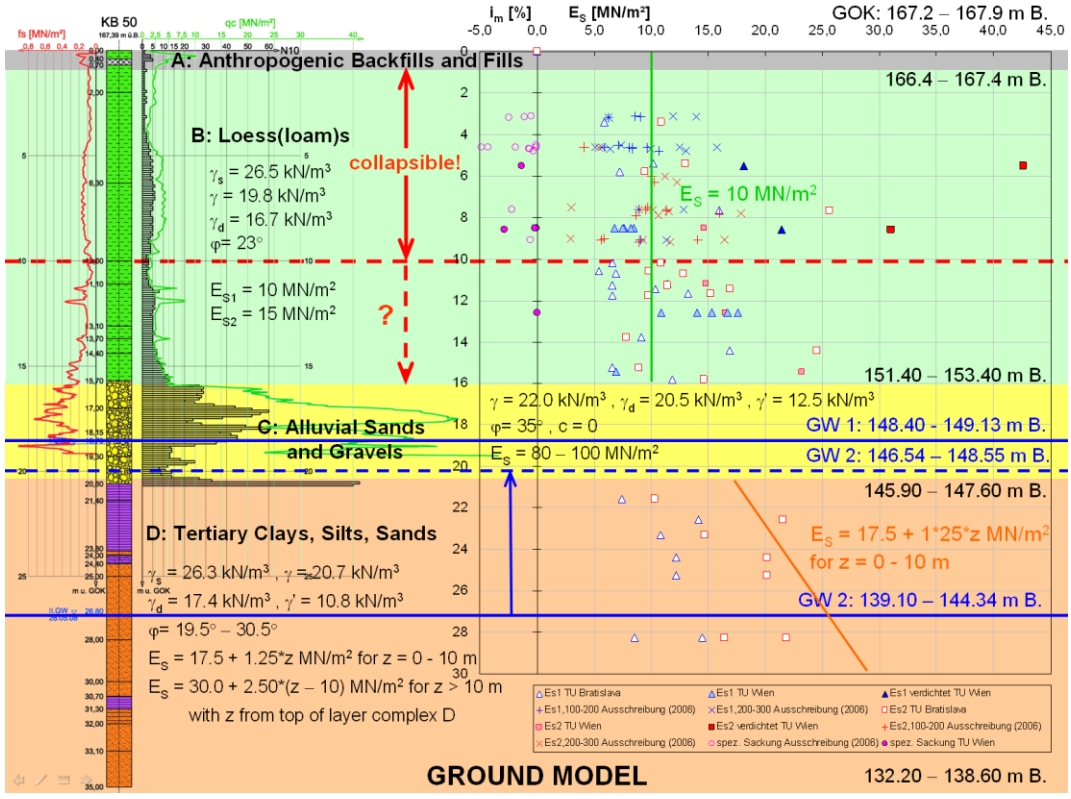


**Figure 15.** Ground model with calculation parameters for each layer.

Under the loess(loam) complex up to a depth of about 20 m to 22 m b.g.l. occur the alluvial sediments in the form of sand, gravel and sand-gravel mixture (layer complex C) with lime concretions up to 80 mm. The upper part the alluvial sediments consist of fine sandy soils which persist clayey-sandy and sporadically fine-grained sands below. In the lower part sandy, well-graded and dense to very dense gravel of high bearing capacity prevails. In some parts of the site at the interface with the underlying gravel, sandstone with a thickness of about 0.3 m was found. From the geotechnical point of view the alluvial gravels are capable of transferring safely and without increased deformations loads several times higher than are the fine soils above.

The underlying stratum made up of tertiary (neogeneous) clays, silts and sands (layer complex D) was found down to the investigated depth of 35 m b.g.l. The tertiary sediments are composed of (clayey-)silty sand, sandy-clayey silt and clay. The plasticity of the cohesive sediments varies from medium (silts) to high and the plastic state from semi-solid to stiff (hard).

The level of the first groundwater table (unconfined groundwater) was at about 19 m b.g.l. in the quaternary sand-gravel layer. Confined groundwater was found between 23 m and 28 m b.g.l. in the water bearing tertiary layers; at the end of the drilling work it welled up to between 19 m and 21 m b.g.l.

It can be summarized that even if the engineering geological conditions of the area from the standpoint of the mode of deposition seems to be relatively simple, the geotechnical conditions are complicated because of the occurrence of loesses susceptible to collapsibility.

### 2.3 *Original foundation concept*

The original foundation concept developed for the heavyweight structures on schematic layouts of the planned power plant comprised the following two foundation methods:

- Original foundation concept A – shallow (spread) foundations on foundation plates (rafts) and, in the case of lightweight structures, on strip footing or on individual columns (pad);
- Original foundation concept B – deep foundation by transferring the entire, mainly dynamic load (action) into the bearing (load resistant) gravelly soils of the layer complex C. It was recommended to transfer the operable load of individual structures by means of wide-section piles embedded on dense or medium dense gravelly soils as the underlying neogeneous clays are characterized by a severalfold lower bearing capacity. Additional investigations revealed that piles had to be embedded deeply within the tertiary sediments, thus pile lengths of about 35 m were necessary due to negative skin friction in the collapsible loess(loam) layer complex.

### 2.4 *Innovative hybrid ground improvement and deep foundation concept*

The foundation measures for the structures of the CCPP 400 MW included deep dynamic compaction in the form of deep dynamic replacement compaction of the subsoil beneath the foundations by the deep vibro replacement technique (VRT) to produce pile-like bearing elements and to improve the soil at depth during the vibration process and stabilization of the soil above the grouted stone columns and stone columns with a lime cement binder (hybrid foundation).

In respect of the static soil pressures, grouted stone columns (foundation concept I) and stone columns (foundation concept II) were produced.

Foundation concept I, which combined the deep vibro replacement technique (VRT) to produce pile-similar bearing elements (grouted stone columns, VSS) with soil stabilization beneath the foundations, was carried out for the heavyweight structures. The area improved by the VSS elements exceeded the slabs by about 2 m on each side. The area of the grid was defined in by the static soil pressure within the following range:

- min. 1.4 m x 1.4 m = 1.96 m²
- max. 2.2 m x 2.2 m = 4.84 m²

The calculated diameter of the grouted stone columns (minimum diameter) was defined as 0.60 m. The thickness of the stabilized soil package varied between about 2 and 3 m.

Foundation concept II, which combined the deep vibro replacement technique (VRT) to produce stone columns (SS) with soil stabilization beneath the foundation slabs, was carried out for lightweight structures. The area improved by the SS elements exceeded the slabs by about 2 m on each side. The area of the grid was defined by the static soil pressure within the following range:

- min. 1.4 m x 1.4 m = 1.96 m²
- max. 2.5 m x 2.5 m = 6.25 m²

The calculated diameter of the stone columns (minimum diameter) was defined with 0.60 m. The thickness of the stabilized soil package was about 2 m.

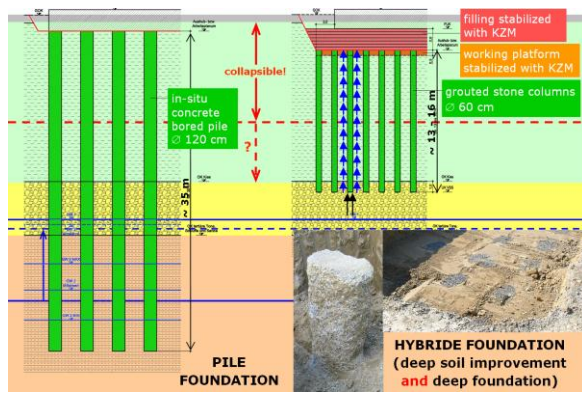


**Figure 16.** Foundation concept with piles (left) vs. hybrid foundation concept based on grouted stone columns (VSS) (right).

Deep vibro replacement was carried out from a working platform that was situated between 2 and 3 m below the bottom of the base slab of the single structures. After the excavation of the soil to the required depth, the excavation level was stabilized with a lime-cement binder to a depth of about 0.5 m. Afterwards the points for the deep vibro replacement process were pre-drilled down to the surface of the quaternary gravel using a continuous flight auger. In the pre-drilled replacement points the grouted stone columns (VSS) or stone columns (SS) were produced

using the deep vibro replacement technique: the gravel was dry fed into the ground and, in the case of grouted stone columns, during the same process mixed in-situ with cement grout. Thus, a solid column was created once the grout h set. The production process allowed the highly flexible and compactable loess around the column to be improved by the horizontally effective dynamically-excited air-fed bottle-like vibrator. Consequently, beside the production of load bearing stone columns the soil was compacted by the vibration process.

### *2.4.1 Soil stabilization*

Both the working platform for the deep vibro replacement method and the fill up to the foundation level were stabilized with a lime-cement mixture (KZM) using the mixed-in-place method.

*Stabilization of the working platform and foundation level*

The excavation was executed to the required depth according to the plan. The excavation level was stabilized with a lime-cement binder (KZM) according to the Geotechnical Report to a depth of about 0.5 m below the excavated level and subsequent dynamic compacting of the working platform. The amount of the KZM mixed in has been determined by a suitability test in the laboratory. The excavation level was stabilized by application of the roller-integrated Continuous Compaction Control (CCC) using a vibratory roller of the type HAMM 3414HT. The stabilized formation level was checked by dynamic load plate tests using the Light Falling Weight Device (LFWD).

If the stabilized excavation level (working platform) beneath the individual structures met the requirements according to the Geotechnical Report (i.e. a dynamic deformation modulus of $E_{vd}$ = 50 MN/m$^2$ proved with the Light Falling Weight Device (LFWD) about 3 days after stabilization and compaction), the subsequent ground improvement works commenced, i.e. the deep vibro replacement works to produce (grouted) stone columns.

*Stabilization of the fill up to the foundation level*

The fill from the level of the working platform up to the formation level of the blinding layer was carried out in layers using the excavated loess (loam) of layer complex B and stabilizing it with a lime-cement binder (KZM) by the mixed-in-place method. After mixing in the required amount of KZM, determined by suitability tests, each layer was compacted dynamically by application of the roller-integrated Continuous Compaction Control (CCC) using a vibratory roller of the type HAMM 3414HT.

Compaction control of each layer was performed with dynamic load plate tests using the Light Falling Weight Device (LFWD).

Finally each stabilized and compacted layer had to meet the requirements according to the Geotechnical Report, i.e. a dynamic deformation modulus of $E_{vd}$ = 75 MN/m$^2$ proved with the Light Falling Weight Device (LFWD) about 3 days after stabilization and compaction.

### *2.4.2 Deep soil replacement – stone columns*

Deep vibro replacement was carried out from the stabilized working platform. The points for the deep vibro replacement process were pre-drilled down to the surface of the quaternary gravel using a continuous flight auger. In the pre-drilled replacement points the stone columns (SS) with a diameter of ≥ 0.6 m were produced using the deep vibro replacement technique.

The principal theoretical background for the calculation of the bearing capacity of a stone column based on Mohr-Coulomb criterion is shown in Figure 18.


**Figure 17.** Deep vibro replacement works.

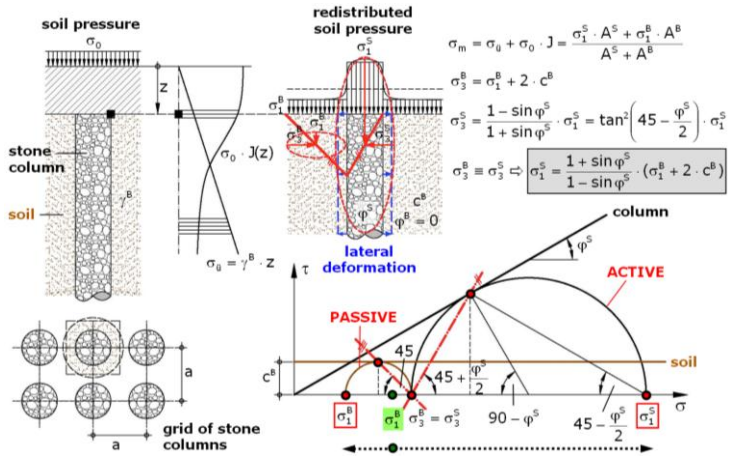


**Figure 18.** Bearing capacity of stone columns.

### 2.4.3 *Deep soil replacement – grouted stone columns*

Deep vibro replacement was carried out from the stabilized working platform. The points for the deep vibro replacement process were pre-drilled down to the surface of the quaternary gravel using a continuous flight auger. In the pre-drilled replacement points (see Figure 19) the grouted stone columns (VSS) were produced using the deep vibro replacement technique. The gravel was dry fed into the ground and during the same process mixed in-situ with cement grout creating solid columns once the grout had set.

The grouted stone columns (VSS) produced with the deep vibro replacement technique (VRT) are similar to unreinforced concrete pile bearing elements. Thus, the analysis of the internal load-bearing capacity of the VSS-element (ultimate limit state design, ULS) has to be done for vertical loads only (without bending moments).

At present a method for the ultimate limit state (ULS) design of grouted stone columns (VSS) is not standardized. Therefore the Austrian standard ÖNORM B 4701 „Concrete structures – EUROCODE-orientated analysis, design and execution“ with partial safety factors (load and resistance factor design, LRFD) has been applied, in which the ULS analysis for unreinforced concrete is regulated according to the Eurocode design concept.

The improvement of the soil around the columns due to the vibration process (anticipation of collapse in the soil structure and compaction) combined with the grouted column material (deep foundation elements) characterizes the hybrid foundation concept resulting in significantly shorter deep foundation elements.

**Figure 19.** Pre-drilled replacement point of the (grouted) stone columns (left) and excavated test column (right).

### 2.5 *Foundation works and quality assurance*

Foundation works (deep soil improvement and deep foundation) took place from December 2008 to April 2009 and had to be performed in a period of heavy snowfall and low temperatures. Nevertheless the deep foundation works were finished within the defined time schedule. Especially for layer-wise stabilization the content of the lime-cement binder determined by a suitability test had to be adapted to the actual weather conditions according to the results of the site control measures. The working platform stabilized with lime-cement by the mixed-in-place

method ensured a continuous execution of the deep vibro replacement works independent of the weather conditions.

The tests and controls performed, and documents produced within the geotechnical supervision of the foundation works (deep vibro replacement method – grouted stone columns and stone columns – and soil stabilization) are summarized in the following sections.

### *2.5.1 Quality control of the deep vibro replacement works*

The production parameters and materials used during the deep vibro replacement process were recorded and documented for each column and point respectively in order to optimize and control the production process. Quality control was accomplished by applying an on-line monitoring system recording:

- energy consumption of the vibrator,
- insertion depth of the vibrator over time,
- production time, and
- material use for each stone column.

The recorded parameters over one day were summarized in a daily report. The documentation records of the deep vibro replacement works were collected on site.

The diameter of the grouted stone columns of 60 cm assumed for the design of the soil improvement measures and the chosen production parameters were verified by producing a test column outside the base slab of the planned structure. After hardening the column was excavated (see Figure 19) and cylindrical specimens were drilled out from the column in order to determine the uniaxial compressive strength. The determined compressive strength exceeded the design value by about 30% to 70%. Uniaxial compression tests to continuously control the production parameters for the deep vibro replacement and to verify the required characteristic value of the compressive cube strength of the material of the VSS element in the ultimate limit state were also performed using specimens that were produced both with cement grout („suspension specimen“) and with gravel-grout compound („mortar specimen“).

A static pile loading test was performed at one test column outside the base slab in order to verify the design load of the grouted stone columns and to get the pile load – deformation relationship.

Vibration measurements were performed during the production of selected grouted stone columns in order to determine the attenuation of the vibrations caused by the deep vibro compaction process.

### *2.5.2 Quality control of the soil stabilization works*

The suitability test of the stabilization of the working platform was determined in-situ at a test field on the basis of dynamic load plate tests using the Light Falling Weight Device (LFWD). The content of the lime-cement binder for the layers of the fill up to the level of the blinding layer was determined on the basis of laboratory tests (suitability tests in the laboratory).

The dynamic compaction of the stabilized working platform and layers of the filling up to the foundation level was carried out by application of the roller-integrated Continuous Compaction Control (CCC) using a vibratory roller of the type HAMM 3414HT.

The compaction control of each layer was performed by with dynamic load plate tests using the Light Falling Weight Device (LFWD).

## 3 SAVA RIVER BRIDGE BELGRADE (SERBIA) DEEP FOUNDATION CONCEPT

### *3.1 Introduction*

Sava Bridge is a 7 span, continuous superstructure with an overall length of 964 m between deck expansion joints (see Figure 20). The main support system is a single pylon asymmetric cable stayed structure with a main span of 376 m and a back span of 200 m. Four spans of 69 m, 108 m, 81 m and 81 m continue the cable stayed section and the end span connecting up the back span is of 50 m length. The pylon is 200 m high. All supports are based on pile foundations. The overall deck width is 45.04 m and shall carry 6 lanes of vehicular traffic, 2 tracks of a new light rail system and 2 lanes of a pedestrian/cycle way.

The conceptual design for the bridge was prepared by Pointing Maribor, DDC Ljubljana and CPV Novi Sad. This concept had to be respected in the detailed design that was to be performed by the contractor (Steinkühler et al. 2010).

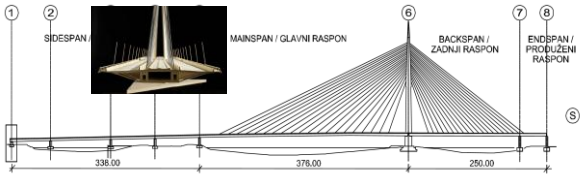


**Figure 20.** Layout of the new bridge over the Sava River in Belgrade and cross section of the bridge deck.

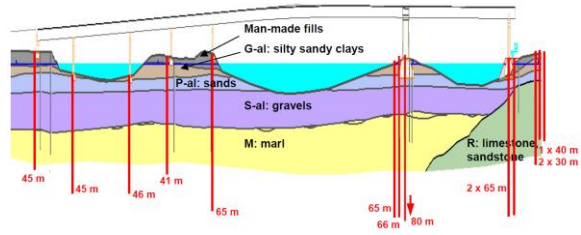


**Figure 21.** Geological longitudinal section (not to scale) and situation of additional exploration borings (red).

In 2007 the company Porr Technobau und Umwelt AG, Austria, was assigned for the construction of the bridge over the Sava River and entrusted both the geotechnical and the structural foundation design to the Foundation Design Consortium, consisting of three Austrian consulting engineers Geotechnik Adam ZT GmbH, Stella and Stengl & Partner, and IBBS Schweighofer. Geotechnical investigation works were done by the Faculty of Mining and Geology of Belgrade University, Serbia, additional soil laboratory tests were performed at the Institute of Geotechnics at Vienna University of Technology, Austria.

### *3.2 Ground conditions*

Referring to reports on interpretation of soil investigations the following geological profile of the ground was derived from 7 boreholes in the conceptual design phase and 13 additional boreholes for detailed design (see Figure 21) (Hinterplattner et al. 2011):

- Layer n : Embankment as artificial surface cover
- Quaternary sediments:
  - Layer G-al: Silty sandy clays with mud interbeds and lenses – facies of flood plain
  - layer P-al: Medium-grained to fine-grained sands – river bed facies
  - Layer S-al: Gravels – river (fluvial) lacustrine sediments
- Tertiary sediments:
  - Layer M: Weathered marly clays and marls and below grey unaltered marls (not registered in boreholes around Piers No. 7 and 8)
  - Layer R: Limestone, sandstones
- Basic geological substratum:
  - Cretaceous sediments

Ground water is strongly influenced by the water level of the Sava River: e.g. at Pier 6 ground water level is 1.48 m above the surface when the river is at high navigation level (HNL) and the subsoil is saturated. When the river is at low navigation level (LNL) the ground water level is at a depth of 2.18 m. In the ground 4 hydro-geological complexes were defined.

Piles for all pier foundations were embedded into the stiff tertiary sediments in order to reduce settlements significantly. Grey unaltered marls have exactly the same textural characteristics as the elevated (roof) weathered marly clays and marls. Their thickness is from 20 to over 30 m. They are characterized by extremely massive texture. Lithological banding is manifested by colour. The increased carbonate content gives the rock a greyish white colour in contrast to the parts with lesser carbonate contents, which are grey. Inclination of lithological banding (bedding) surface amounts to around 3° to 5°. The lithological banding surfaces, especially when they are encountered in the form of thin "film" of sandy mass, represent latent mechanical discontinuities. They are overconsolidated and hard with conchoidal rupture. The marls are poorly compressible and are practically impermeable. In relation to physical-mechanical properties, at the scale of mm to cm observations, they represent a poorly heterogeneous and anisotropic environment, whereas in the larger metre scale observation area they are practically homogenous and isotropic. These tertiary sediments were generally explored except in boreholes in the area of Piers 7 and 8 (see Piers 6 and 7 in Figure 22).

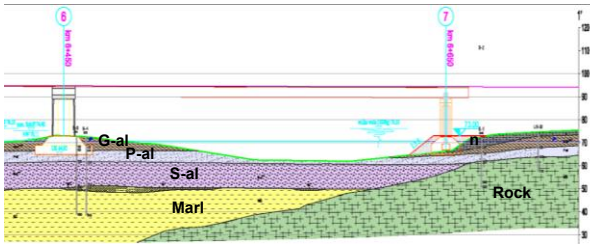


**Figure 22.** Different geological situation in the area of Pier 6 and Pier 7.

Limestone is of Sarmatian age and is represented by sandy phytogenous detritus full of fauna in places with fossilized mollusc lumachelle. Because of karstification this phytogenous rarely sandy limestone (calcarenite) is riddled with caverns and fractures of various sizes and in the near-surface area mostly filled with material from the elevated (roof) stratum. Their structure is massive and in certain parts brecciate. Thicknesses vary from several meters to several tens of meters. They are usually encountered under grey marls. Their contact with underlying Cretaceous sediments is discordant.

Cretaceous sediments represent the basic geological substratum of the ground. Most of the flysch is composed of sandstones, which alternates with siltstones and clayey shale. Micro conglomerates are rarely encountered.

### *3.3 Soil parameters*

Based on the ground exploration and soil investigations undertaken, calculation parameters for geotechnical design were derived in particular from laboratory tests performed in the conceptual design phase and in the detailed design phase at Belgrade University and Vienna University of Technology. The particular laboratory tests have been concluded in tables and analysed statistically (Geotechnik Adam ZT GmbH 2009a,b,c). The following characteristic soil parameters were derived from statistical evaluation, empirical data and cautious selection with engineering judgment (Tables 3 and 4).

**Table 3:** Characteristics soil parameters for geotechnical design (Geotechnik Adam ZT GmbH 2009a,b,c).

| layer | description (unified classification (USCS)) | weight density $\gamma$ | effective weight density $\gamma'$ | saturated weight density $\gamma_{sat}$ | effective shear angle $\varphi'$ | cohesion c | oedometer modulus $E_{oed}$ | deformation modulus $E_d$ |
|---|---|---|---|---|---|---|---|---|
| | | [kN/m³] | [kN/m³] | [kN/m³] | [°] | [kN/m²] | [MN/m²] | [MN/m²] |
| **n** | Embankment | 19.5 | 10.0 | 20.0 | 25 | 0 | n.r. | n.r. |
| **G-al** | Silty-sandy clays with mud interbeds and lenses (CL, CH, MH) | 18.5 | 8.5 | 18.5 | 25 | 0 | 2 | n.r. |
| **P-al** | Medium-grained to fine-grained sands – river bed facies (SU) | 18.5 | 9.0 | 19.0 | 30 | 0 | 10 | n.r. |
| **S-al** | Gravels – River (fluvial)- lacustrine sediments (GP) | 22.5 | 12.5 | 22.5 | 35 | 0 | 30 | n.r. |
| **M- lg,l*** | Weathered marly clays and marls | 18.0 | 8.5 | 18.5 | 25 | 0 | 25 | n.r. |
| **M-L** | Grey unaltered marls | 18.5 | 9.0 | 19.0 | 30 | 20 | 60 - 100 | n.r. |
| **M-K** | Limestone (rock monolith) | 22.0 | n.r. | n.r. | n.r. | n.r. | n.r. | ≥ 2000 |
| **M-ps** | Sandstone (rock monolith) | 25.0 | n.r. | n.r. | n.r. | n.r. | n.r. | ≥ 8000 |
| **K** | Cretaceous sediments | n.r. | n.r. | n.r. | n.r. | n.r. | n.r. | n.r. |

**Table 4:** Characteristic soil parameters for derivation of shaft friction and base resistance pressure according to technical provisions (Geotechnik Adam ZT GmbH 2009a,b,c).

| layer | Description | undrained shear strength $c_u$ | cone penetration resistance (CPT) $q_c$ | uniaxial compression strength $q_u$ | number of blows (SPT) N |
|---|---|---|---|---|---|
| | | [kN/m²] | [MN/m²] | [kN/m²] | [-] |
| **n** | Embankment | - | 1 | - | 3 |
| **G-al** | Silty-sandy clays with mud interbeds and lenses | - | 1 | - | 3 |
| **P-al** | Medium-grained to fine-grained sands - river bed facies | - | 5 | - | 15 |
| **S-al** | Gravels – River (fluvial)- lacustrine sediments | - | 15 | - | 45 |
| **M- lg,l•** | Weathered marly clays and marls | 200 | 3 | 400 | - |
| **M-L** | Grey unaltered marls | 900 | 11 | 1800 | - |
| **M-K** | Limestone (rock monolith) | - | - | ≥ 1000 | - |
| **M-ps** | Sandstone (rock monolith) | - | - | ≥ 5000 | - |
| **K** | Cretaceous sediments | - | - | - | - |

### *3.4 Deep foundation design concept*

#### *3.4.1 Design concept for pile group foundations of Piers 1 to 5 and Piers 7 and 8*

Pile group foundations at Piers 1 to 5 as well as Piers 7 and 8 are composed of single piles with a defined spacing between the piles forming pile groups. The bearing capacity of a single pile consists of the total shaft resistance (derived from shaft friction) and the activated base resistance force (derived from base resistance). Overall bearing capacity of a pile group foundation depends on the pile spacing as well and therefore has to be taken into account. Pile spacing had to be e ≥ 2.5 D otherwise a reduction of shear parameters was necessary.

Verification of vertical bearing capacity was performed according to EN 1997-1 (EC7 2006). The partial safety factors were assessed according to the national specifications concerning ÖNORM EN 1997-1 (2006) and national supplements. Table 5a and 5b contain the partial safety factors and correlation factors to evaluate the results of static pile load tests according to ÖNORM B 1997-1-1 (2007) for the design of the pile foundations.

**Table 5a:** Partial safety factors and correlation factors to evaluate the results of static pile load tests according to ÖNORM B 1997-1-1 (2007) (this code with national specifications and national supplements is not available in English language; translated by the author).

*Table 5: Partial safety factors on the effects of actions ($\gamma_E$)*

| action | | symbol | value | | |
|---|---|---|---|---|---|
| duration | condition | | BS 1 | BS 2 | BS 3 |
| permanent | unfavourable | $\gamma_G$ | 1.35 | 1.20 | 1.00 |
| | favourable | $\gamma_G$ | 1.00 | 1.00 | 1.00 |
| variable | unfavourable | $\gamma_Q$ | 1.50 | 1.30 | 1.00 |

*Table 6: Partial safety factors for soil parameters ($\gamma_M$)*

| soil parameter | symbol | value |
|---|---|---|
| angle of shearing resistance [a] | $\gamma_{\varphi'}$ | 1.00 |
| effective cohesion | $\gamma_{C'}$ | 1.00 |
| undrained shear strength | $\gamma_{cu}$ | 1.00 |
| unconfined strength | $\gamma_{qu}$ | 1.00 |
| weight density | $\gamma_\gamma$ | 1.00 |
| [a]) this factor is applied to tan φ' | | |

**Table 5b:** Partial safety factors and correlation factors to evaluate the results of static pile load tests according to ÖNORM B 1997-1-1 (2007) (this code with national specifications and national supplements is not available in English language; translated by the author).

*Table 7: Partial resistance factors ($\gamma_R$) for driven piles, bored piles and continuous flight auger piles*

| **resistance** | **symbol** | **value** |
|---|---|---|
| base | $\gamma_b$ | 1.10 |
| shaft (compression) | $\gamma_s$ | 1.10 |
| total/combined (compression) | $\gamma_t$ | 1.10 |
| shaft in tension | $\gamma_{s;t}$ | 1.15 |

*Table 8: Correlation factors ($\xi$) to derive characteristic values from static pile load tests*

| **ξ for n =** | **1** | **2** | **3** | **4** | **≥ 5** |
|---|---|---|---|---|---|
| $\xi_1$ | 1.40 | 1.30 | 1.20 | 1.10 | 1.00 |
| $\xi_2$ | 1.40 | 1.20 | 1.05 | 1.00 | 1.00 |
| n number of tested piles | | | | | |

In the scope of the objective of the project no tension piles were expected so that an overall valid partial safety factor was assessed according to ÖNORM B 1997-1-1, Table 7 (2007):

$$\gamma_R = 1.10$$

At Piers 5, 6 and 7 pile load tests were carried out. By means of the comparable stratigraphy of the ground at Piers 1 to 6 the results of pile load tests at Piers 5 and 6 could be transferred to Piers 1 to 4 as well. Consequently, the following spreading factors were selected according to ÖNORM B 1997-1-1 Table 8:

$$\xi_1 = 1.40 \ (n = 1)$$
$$\xi_2 = 1.40 \ (n = 1)$$

### *3.4.2 Design concept for the box-shaped foundation of the pylon at Pier 6*

The box-shaped foundation beneath pylon at Pier 6 is composed of a compound body consisting of an encasing diaphragm wall and piles as well as the enclosed soil. This quasi-monolith transfers high vertical and horizontal forces. Piles and capping raft form a box, which acts physically like a "pot" turned upside down. Consequently, the settlements are smaller than for conventional pile groups, and the earthquake resistance is significantly higher. Box-shaped foundations represent a special form of piled raft foundations utilising the enclosed soil core as an integrated load transfer member.

The following two calculation models were applied. They have proved satisfactory in the design of several bridges over the river Danube in Austria (Fross et al. 2010).

*Calculation model A: single piles and diaphragm wall*

- Evaluating the bearing capacity of single elements they provided only fictitious limit case values because the bond effect between concrete elements and enclosed soil core was neglected. Thus, maximum pile or diaphragm wall loads were calculated.
- Verification of vertical bearing capacity was performed according to EN 1997-1 (EC 7).
- Shaft friction was taken into account at outer and inner box surfaces (including the pile rows) and base resistance forces of the single piles and the diaphragm wall.

*Calculation model B: quasi-monolithic*

- According to Brandl (2003) a full bond effect between deep foundation elements and the closed soil was assumed. This compound body comprises the outer circumference of the foundation, if secant piles or diaphragm walls are installed. In the case of contiguous piles the theoretical area should be reduced by at least half a pile diameter. For the quasi-monolith, only shaft friction along the outside surface of the foundation box may be taken into account.
- The monolith-theory provides minimum pile or diaphragm wall loads. However, a full composite effect occurs only theoretically but hardly in practice. Therefore, relatively high safety factors are required. According to Brandl (2003) calculations should be based on a global safety factor of $\eta \geq 3.0$, if conventional calculation methods for evaluating the base failure of equivalent "shallow" foundations are used.
- According to Brandl (2003) a global safety factor of ground failure of the raft foundation for river bridge foundations of $\eta = 3.5$ was used.

- Shaft friction is effective only around the outer perimeter of the box-shaped foundation.
- The base pressure was assumed to be effective over the entire base area of the monolith. The base pressure should not exceed the actual overburden stress multiplied by the over consolidation ratio (OCR) of the marl in order to minimize foundation settlements and differential settlements. OCR was determined with particular tests in the scope of laboratory investigations. Taking into account an average weight of soil of 20 kN/m² OCR ranges from 950 to 1,940 kN/m² at the bridge site.

*Seismic foundation design*

For seismic design two approaches were considered:

On the one hand dynamic soil parameters can be determined from geophysical field tests (e.g. cross-hole and down-hole tests) and/or dynamic laboratory tests (e.g. resonant columns test). Field tests deliver elastic data (dynamic shear modulus and dynamic elastic modulus) at small shear strains. However, increasing shear strains produce a reduction of the dynamic stiffness parameters. Depending on the seismic load and the corresponding shear strain the dynamic parameters can be identified. The stiffness and damping matrices can be determined by using a suitable model, whereby radiation damping is represented by the damping matrix. However, radiation damping is always beneficial for the structure, thus neglecting this effect gives a solution on the safe side.

On the other hand seismic calculations can be performed by variation of the static stiffness, if radiation damping can be neglected. In general, the quasi-static stiffness increases when dynamic loads are applied.

In the scope of the seismic design of the foundations of the Sava Bridge parametric studies were performed taking into account both approaches. Dynamic soil parameters were derived from geophysical tests and data given by the Serbian Seismic Institute in Belgrade. A comparison of dynamic and quasi-static solutions suggested that the dynamic approach overestimated the spring stiffness by means of the assumed rigid foundation behaviour during seismic load because the overall stiffness of the system was limited by the inherent rigidity of the foundation itself. Thus, the following parameters were chosen from the parametric studies:

- Lower limit: static value of horizontal and vertical modulus of subgrade reaction
- Upper limit: 10 times the static value of horizontal and vertical modulus of subgrade reaction

Characteristic values for shaft resistance and base resistance pressure did not need to be modified from static values. Consequently, the ground is stiffer at lower strains during an earthquake, thus causing higher reaction forces but lower deformations. A softening of the ground can be excluded since the expected shear strains in the soil are small taking into account the magnitude of a presumed earthquake and the liquefaction potential of the layered ground is negligible (Geotechnik Adam ZT GmbH 2009a,b,c).

### *3.4.3 Geotechnical design parameters*

For calculation and both static and seismic design of bored piles and diaphragm walls the following geotechnical soil parameters were specified for each pier:

- Shaft friction.
- Base resistance pressure.
- Horizontal subgrade reaction.
- Vertical subgrade reaction.

*Shaft friction and base resistance pressure*

ÖNORM EN 1997-1 (EC 7 2006) includes no specifications related to the definition of shaft friction and base resistance pressure. For that reason other technical provisions need to be stressed. Hitherto in Austria ÖNORM B 4440 (2001) has been used for the determination of design axial pile loads according to the global safety concept including the design base resistance pressure and the design shaft friction. In contrary the ÖNORM EN 1997-1 (EC 7 2006) is based on the partial safety concept so that design values defined in ÖNORM B 4440 (2001) cannot be directly adopted for applications according to the partial safety concept.

ÖNORM B 1997-1-3 (draft, 2007) is currently established by the Austrian Standard Institute. The new standard will replace ÖNORM B 4440 (2001) and will cover all pile types. Amongst others procedures for determination of characteristic values for ultimate limit state (ULS) and serviceability limit state (SLS) will be defined in tables including the base resistance pressure and shaft resistance (see Tables 4, 5 and 6).

The design value of pile resistance $R_{c;d}$ for a bored pile at pressure is defined by:

$$R_{c;d} = R_{c;k} / (\gamma_t \, . \, \eta_{P;c}) \qquad (1)$$

with

$\gamma_t$: partial safety factor of pile resistance; according to ÖNORM B 1997-1-1 Table 7: $\gamma_t = 1.10$.

$\eta_{P;c}$: scale factor (model factor) for axially loaded piles at pressure; according to ÖNORM B 1997-1-3 (draft) Table A.5 resp. ÖNORM B 1997-1-1: $\eta_{P;c} = 1.30$.

$R_{c;k}$: characteristic pile resistance as a result of shaft resistance and base resistance pressure; according to ÖNORM B 1997-1-3 (draft) Table C.4 to C.7.

**Table 6a:** Tables from new ÖNORM B 1997-1-3 (draft October 2007; this draft is not available in English language; translated by the author).

*Table A.5: scale factors (model factors) (η)*

| case | symbol | value |
|---|---|---|
| resistances of static pile load tests (axial compression) | $\eta_{P;c}$ | 1.0 |
| resistances of static pile load tests (axial tension) | $\eta_{P;t}$ | 1.0 |
| resistances of the tables of annex C and D (axial compression) | $\eta_{P;c}$ | 1.3 |
| resistances of the tables of annex C and D (axial tension) | $\eta_{P;t}$ | 2.5 |
| box shaped foundation | $\eta_{KG}$ | ? * |
| combined raft-pile foundation | $\eta_{KPP}$ | ? * |

*Table C.1: Coherences between SPT results in the borehole and density index of coarse grained soils and between consistency index and condition of fine grained soils*

| **coarse grained soil** | |
|---|---|
| **SPT number of blows $N_{30}$ (penetration of 30cm)** | **density index** |
| 0 to 4 | very loose |
| more than 4 to 10 | loose |
| more than 10 to 30 | medium dense |
| more than 30 to 50 | dense |
| more than 50 | very dense |

*Table C.1 continued*

| **fine grained soil** | |
|---|---|
| **consistency index** $I_c = \frac{w_l - w}{I_p}$ | **condition** |
| 0.0 to 0.25 | pappy |
| more than 0.25 to 0.50 | very soft |
| more than 0.50 to 0.75 | soft |
| more than 0.75 to 1.00 | firm |
| more than1.00 | semi hard |

*Table C.2: Minimum embedding depth in coarse soil layers of low plasticity*

| density index | SPT number of blows $N_{30}$ | minimum embedding depth $l_{min}$ |
|---|---|---|
| very dense | more than 50 | d |
| dense | more than 30 to 50 | 2 d |
| medium dense | more than 10 to 30 | 3 d |

*Table C.3: Minimum embedding depth in fine grained soil layers of low plasticity*

| consistency | minimum embedding depth $l_{min}$ |
|---|---|
| semi hard to hard | d |
| firm | 2 d |

*Table C.4: Characteristic base resistance of piles ($q_{b;k}$) in coarse grained (non-cohesive) soils, depending on N30 -values (SPT)*

| **specific settlement of pile cap $s/D_b$** | **characteristic base resistance of piles ($q_{b;k}$) in widely grained sand and sand-gravel mixtures** | | |
|---|---|---|---|
| | **medium dense [1])** | **dense [2])** | **very dense [3])** |
| | **MN/m²** | **MN/m²** | **MN/m²** |
| 0.005 | 0.30 | 0.40 | 0.50 |
| 0.01 | 0.55 | 0.80 | 1.00 |
| 0.02 | 1.05 | 1.40 | 1.75 |
| 0.03 | 1.35 | 1.80 | 2.25 |
| 0.05 | 1.90 | 2.50 | 2.95 |
| 0.075 | 2.50 | 3.10 | 3.55 |
| 0.10 (=$s_g$) | 3.00 | 3.50 | 4.00 |

[1]) $N_{30}$ -value ≥ 10
[2]) $N_{30}$ -value ≥ 30
[3]) $N_{30}$ -value ≥ 50
Intermediate values may be obtained by linear interpolation

**Table 6b:** Tables from new ÖNORM B 1997-1-3 (draft October 2007; this draft is not available in English language; translated by the author).

*Table C.5: Characteristic base resistance of piles ($q_{b;k}$) in fine grained (cohesive) soils, depending on consistency index $I_c$*

| **specific settlement of pile cap $s/D_b$** | **Characteristic base resistance of piles ($q_{b;k}$) in silt, clayey silt and clay** | | |
|---|---|---|---|
| | **stiff [1])** | **very stiff [2])** | **semi solid [3])** |
| | **MN/m²** | **MN/m²** | **MN/m²** |
| 0.005 | 0.10 | 0.15 | 0.25 |
| 0.01 | 0.15 | 0.30 | 0.45 |
| 0.02 | 0.35 | 0.60 | 0.90 |
| 0.03 | 0.45 | 0.80 | 1.15 |
| 0.05 | 0.60 | 1.10 | 1.60 |
| 0.075 | 0.70 | 1.40 | 2.00 |
| 0.10 (s = $s_g$) | 0.80 | 1.50 | 2.20 |
| [1]) $I_c \geq 0.75$<br>[2]) $I_c \geq 0.90$<br>[3]) $I_c > 1.00$<br>Intermediate values may be obtained by linear interpolation | | | |

*Table C.7: Characteristic shaft resistance of piles ($q_{s;k}$) in fine grained (cohesive) soils, depending on consistency index $I_c$ respectively on unconfined compressive strength $q_u$*

| **specific settlement of pile cap $s/D_b$** | **Characteristic base resistance of piles ($q_{b;k}$) in silt, clayey silt and clay** | | |
|---|---|---|---|
| | **stiff [1])** | **very stiff [2])** | **semi solid [3])** |
| | **MN/m²** | **MN/m²** | **MN/m²** |
| 0.005 | 0.10 | 0.15 | 0.25 |
| 0.01 | 0.15 | 0.30 | 0.45 |
| 0.02 | 0.35 | 0.60 | 0.90 |
| 0.03 | 0.45 | 0.80 | 1.15 |
| 0.05 | 0.60 | 1.10 | 1.60 |
| 0.075 | 0.70 | 1.40 | 2.00 |
| 0.10 (s = $s_g$) | 0.80 | 1.50 | 2.20 |
| [1]) $I_c \geq 0.75$<br>[2]) $I_c \geq 0.90$<br>[3]) $I_c > 1.00$<br>Intermediate values may be obtained by linear interpolation | | | |

*Table C.6: Characteristic shaft resistance of piles ($q_{s;k}$) in coarse grained (non-cohesive) soils, depending on N30-values (SPT)*

| **coarse grained soils** | | **characteristic shaft resistance ($q_{s;k}$)** | |
|---|---|---|---|
| | | **for serviceable limit state SLS** | **for ultimate limit state ULS** |
| **density index** | **$N_{30}$-value (SPT)** | **MN/m²** | **MN/m²** |
| loose | 4 | 0.030 | 0.045 |
| medium dense | 10 | 0.050 | 0.075 |
| | 20 | 0.060 | 0.090 |
| dense | 30 | 0.070 | 0.105 |
| | 40 | 0.095 | 0.142 |
| very dense | ≥ 50 | 0.120 | 0.180 |
| Intermediate values may be obtained by linear interpolation | | | |

The characteristic values for shaft resistance and base resistance pressure of piles in soil given in the following were specified based on the results of ground investigations and empirical values, which have already been adopted in the draft version of ÖNORM B 1997-1-3 (draft, 2007). The characteristic values for shaft resistance and base resistance pressure of piles in rock (limestone and sandstone at Pier 7) were specified according to DIN 1045 – Appendix B, Table B.5 (2005) (failure values).

For geotechnical design of the pile group foundations at Piers 1 to 5 and the box-shaped foundation at Pier 6 characteristic values for shaft friction and base resistance pressure given in Table 7 were derived (Geotechnik Adam ZT GmbH 2009a,b,c).

**Table 7:** Characteristic values of shaft friction and base resistance pressure of single piles.

| **layer** | **description** | **shaft friction $q_{s,k}$ [kN/m²]** | **base resistance pressure $q_{b,k}$ [kN/m²]** | | |
|---|---|---|---|---|---|
| | | | **s/D= 0.02** | **s/D= 0.03** | **s/D= 0.05** |
| **P-al** | Medium-grained to fine-grained sands - river bed facies | 40 | - | - | - |
| **S-al** | Gravels – River (fluvial)- lacustrine sediments | 140 | - | | |
| **M-lg,l•** | Weathered marly clays and marls | 60 | - | - | - |
| **M** | Grey unaltered marls | 80 | 900 | 1,150 | 1,600 |
| **M-K** | Limestone | 126 | 1,880 | | |

The pile foot was embedded within sound marl; the vertical modulus of subgrade reaction was defined in the following range taking into account the single pile load, the stiffness modulus of the soil, and the expected settlement:

$$k_{S,V} = 75 – 83 \text{ MN/m}^3 \quad (2)$$

For the design of the pile foundation the distribution of the horizontal modulus of subgrade reaction presented in Table 8 was applied, which was determined from SPT, CPT, and further ground investigation (Geotechnik Adam ZT GmbH 2009a,b,c).

**Table 8:** Horizontal modulus of subgrade reaction.

| depth | modulus of horizontal subgrade reaction | distribution of modulus of horizontal subgrade reaction |
|---|---|---|
| above top of layer P-al | 0 MN/m³ | linear |
| bottom of layer P-al | 25 MN/m³ | |
| top of laver S-al | 50 MN/m³ | linear |
| bottom of laver S-al | 100 MN/m³ | |
| top of weathered marl M- lg,l* | 100 MN/m³ | constant |
| bottom of weathered marl M- lg,l* | 100 MN/m³ | |
| below top of grey unaltered marls M | 150 MN/m³ | constant |

**Table 9:** Characteristic values of shaft friction and base resistance pressure of single piles. Rock values according to DIN 1054 (2005).

| layer | description | shaft friction $q_{s,k}$ [kN/m²] | base resistance pressure $q_{b,k}$ [kN/m²] | | |
|---|---|---|---|---|---|
| | | | s/D= 0.02 | s/D= 0.03 | s/D= 0.1 |
| **G-al** | Silty-sandy clays with mud interbeds and lenses | 0 | - | - | - |
| **P-al** | Medium-grained to fine-grained sands - river bed facies | 0 | - | - | - |
| **S-al** | Gravels – River (fluvial)- lacustrine sediments | 0 | - | | |
| **M-K** | Limestone | 126 | - | | |
| **M-ps** | Sandstone | 500 | 5,000 | | |

At Piers 7 and 8 the rock surface was found in a depth of about 17 m below actual ground surface; thus tip resistance piles (end bearing piles) had to be used. For geotechnical design of the pile foundation (pile group) characteristic values for shaft friction and base resistance pressure (see Table 9) were applied (Geotechnik Adam ZT GmbH 2009a,b,c).

If the pile foot was embedded within the sound rock, the vertical modulus of subgrade reaction was defined in the following range taking into account the single pile load, the stiffness modulus of the soil, and the expected settlement:

$$k_{S,V} = 1{,}000 \text{ MN/m}^3 \quad (3)$$

For the design of the pile foundation the distribution of the horizontal modulus of subgrade reaction presented in Table 10 was applied, which has been determined from SPT, CPT, and further ground investigation (Geotechnik Adam ZT GmbH 2009a,b,c).

**Table 10:** Horizontal modulus of subgrade reaction.

| depth | modulus of horizontal subgrade reaction | distribution of modulus of horizontal subgrade reaction |
|---|---|---|
| above top of layer M-K | 0 MN/m³ | - |
| top of laver M-K | 100 MN/m³ | linear |
| bottom of laver M-K | 200 MN/m³ | |
| below top of laver M-ps | 500 MN/m³ | constant |

The following additional specifications had to be considered:

- Overall bearing capacity of a pile group foundation depends on the pile spacing as well and therefore has to be taken into account. Pile spacing has to be $e \geq 2.5 \cdot D$, otherwise a reduction of shear parameters has to be performed.
- Distance of excavation level to bedding zone has to be $\geq 3.0$ m.
- Horizontal stresses in the bedding zone must not exceed the passive earth pressure.
- Group factors $\alpha_L$ and $\alpha_Q$ according to DIN 1054 have to be considered.
- According to DIN 1054 (2005) and ÖNORM B 1997-1-3 (draft, 2007) a minimum embedding depth in the sound marl of $t_E \geq 5$ m has to be taken into account.

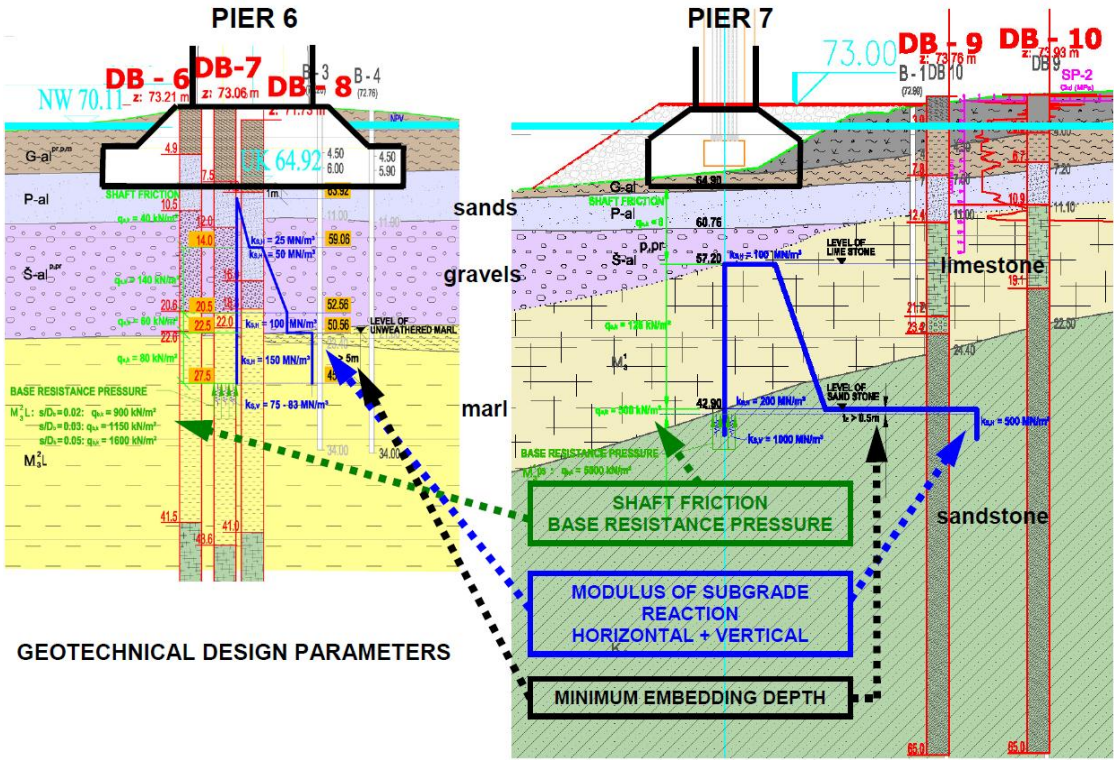


**Figure 23.** Geotechnical design parameters exemplary for Pier 6 (left) and Pier 7 (right).

In Figure 23 the geotechnical design parameters derived from the soil parameters take into account the applied standards according to EC 7 (2006) are illustrated for Pier 6 (box-shaped foundation embedded in marl) and Pier 7 (pile group foundation embedded in rock).

### *3.5 Box-shaped foundation for the pylon at Pier 6*

#### *3.5.1 Layout and calculation model for box-shaped foundation*

In the following the box-shaped foundation for the pylon at Pier 6 is described in more detail. It consists of an encasing diaphragm wall and piles inside (see Figure 24):

- Piles: 113 piles with a diameter of 1.5 m
- Pile length: 29.0 m
- Diaphragm wall: thickness of 1.0 m, length of 37 m
- Pile cap: diameter of 25.0, 30.0 and 34.0 m and a total thickness of 8.0 m

The total load (serviceability limit state) amounted to 602 MN, whereas dead load of piles, diaphragm wall and pile cap were not included. The maximum working load of a single pile was 3.7 MN. Taking into account the additional load due to the dead load of the pile raft (uplift is considered for ground water level at low navigation level) the maximum working load of a single pile amounted to 4.4 MN (Hinterplattner et al. 2011).

Compared to the original conceptual design a reduction of the number of piles could be achieved. The encasing diaphragm wall additionally served as a retaining wall for the construction pit of the pile raft. Thus, no additional measures were necessary to secure the construction pit against earth pressure, traffic loads and water pressure in particular in case of floods.

The calculation model for the foundation substructure illustrated in Figure 25 was established by considering the geometry and the stiffness of the foundation elements (diaphragm wall, piles, and pile raft).

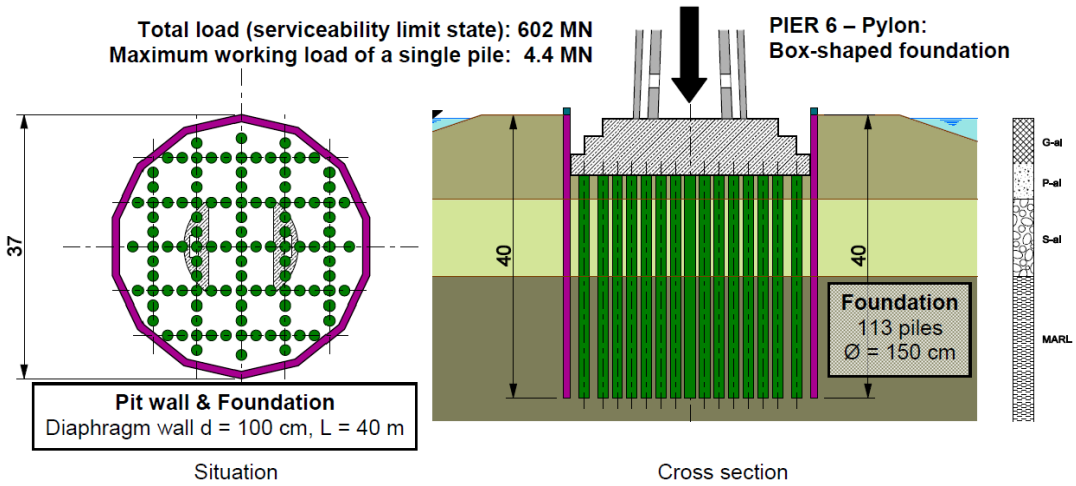


**Figure 24.** Layout of the box-shaped foundation for the pylon at Pier 6.

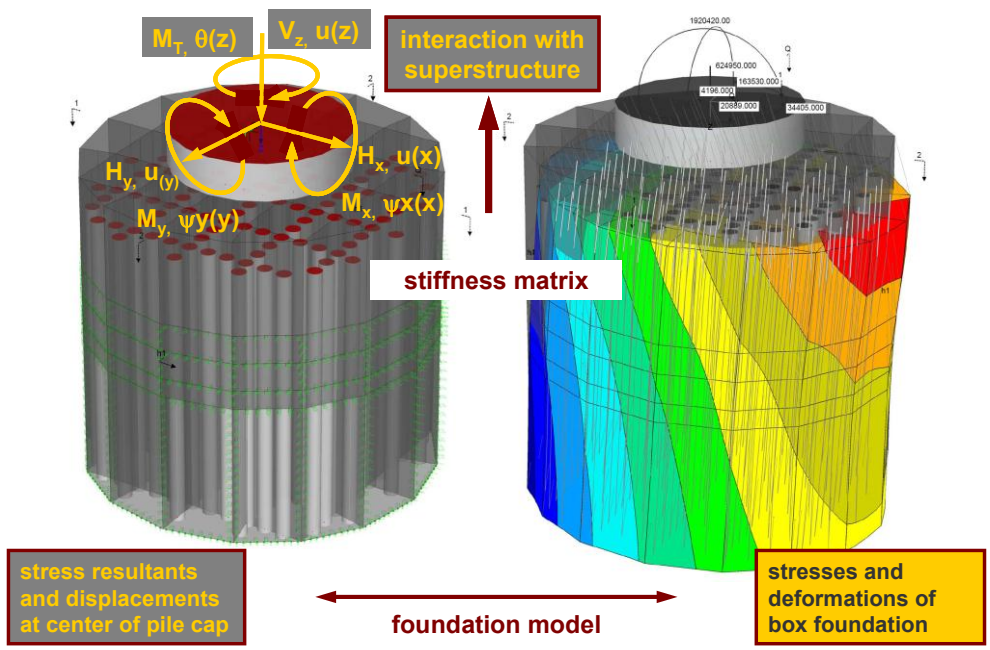


**Figure 25.** Calculation model for boxed-shaped foundation of pylon at Pier 6 and stiffness matrix.

The ground reaction was derived from the horizontal and the vertical modulus of subgrade reaction to be effective at the base and the vertical diaphragm panels.

The stress resultant components ($V_z$, $H_x$, $H_y$; $M_x$, My, MT) and both the displacement ($u_x$, $u_y$, $u_z$) and the rotation/torsion components ($\psi x_x$, $\psi y_y$, $\theta_z$) (in total resulting in 6 degrees of freedom) were calculated

for a unit load at the top centre of the pile raft in order to derive the stiffness matrix of the box-shaped foundation compound interacting with the bridge superstructure. Stresses and deformations were then determined applying the substructure technique coupling the foundations of all piers with the bridge superstructure.

### *3.5.2 Trial piles*

In order to verify the soil parameters used for the calculation and design of the Sava Bridge pile foundations, four trial piles at Piers 5, 6 and 7 were installed and tested. The test load was assessed as the working load multiplied by a safety factor of 2.125 according to EC 7-1 (design situation BS1).

As an example Figure 26 shows measurement results of trial pile No. 2, situated at Pier 6, with a diameter of 1.5 m, a length of 38.1 m and a maximum test load of 9.6 MN (considering a working load of 4.4 MN). Up to a depth of 8 m, which corresponds to a depth of the designed pile raft, an elimination pipe was installed in order to avoid skin friction within the upper soil layers. At the maximum load stage measured settlements were 7.3 mm, with a plastic portion of 2.7 mm. The ratio of settlement to pile diameter was s/D = 0.0049 related to total settlements. The measurement results have shown that a base resistance of $q_b$ = 122 kN/m² (equates to 216 kN) occurred at the maximum load stage. The average skin friction within sand layers (P-al) and gravel layers (S-al) and marl (M) was approx. $q_s$ = 56 kN/m².

By means of measurement results (particularly with regard to measured deformation) it was assumed that the ultimate limit state was not reached with the test load of 9.6 MN. This means, that the bearing capacity was higher than the test load.

Hence, bearing capacity was better than expected. Due to rock-similar behaviour of marls, skin friction within layers P-al and S-al (both granular soil) was mobilised to a minor extent only, because of low vertical deformations. Although the ultimate bearing capacity, base resistance and skin friction of each single layer could not be determined by pile load tests, it was proven that the intended workloads could be transferred to the ground with low deformations and sufficient safety. Thus, design parameters (Geotechnik Adam ZT GmbH 2009a,b,c) were approved and could be used for design of pile foundations.

Finally, the results of these trial piles also provided information about the settlements of a single pile and were applied for settlement calculations.

### *3.6 Settlements*

Foundations also were designed for the serviceability limit state (SLS) so that calculated settlements met the requirements derived from the allowable deformations of the superstructure. According to Brandl (2005) for settlement analyses the monolith-

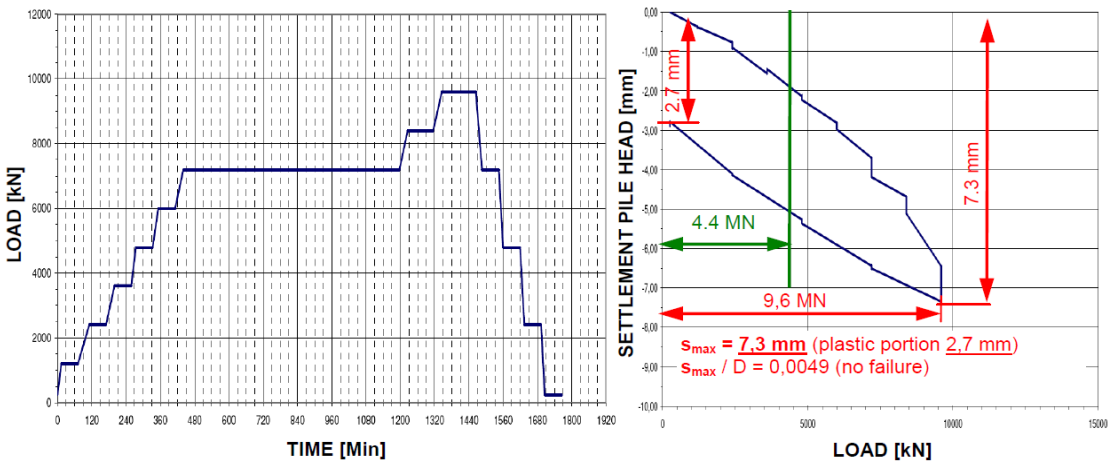


**Figure 26.** Results of axial static pile load test at Pier 6; maximum test load of 9.6 MN with a maximum working load of 4.4 MN (Bauer Spezialtiefbau GmbH 2009).

theory has proved practicable and sufficiently accurate in engineering practice by assuming the base of the box-foundation as the fictitious surface in the half space. The theoretical contact pressure included the reduction of the total load Q by the shaft friction $Q_s$.

In the static model of the superstructure a stiffness matrix was integrated at each pier in order to consider the pile foundation. Furthermore, additional differential settlement Δs with ±1.0 cm (|Δs| = 2.0 cm) was considered at each support using the elastic stiffness of the structure, whereas at the pylon axis a settlement Δs of 5.0 cm and a rotation Δφ of ±1.0‰ were considered. Due to ground conditions at Piers 7 and 8 (rock) and the results of trial piles differential settlement Δs with ± 0.5 cm (|Δs| = 1.0 cm) was assumed for the axes 7 and 8.

In order to check the assumptions settlement calculations with the static model of the superstructure have been performed. The foundation of the piers is within rock-like marl at Piers 1 to 6 and within sandstone at Piers 7 and 8. Therefore, the piles predominantly work as end bearing piles. The total settlements ($s_{total}$) of the foundation consist of the settlements of the single piles ($s_1$) as well as the settlements of the pile group ($s_2$) (DIN 1054 2005):

$$s_{total} = s_1 + s_2 \quad (4)$$

The settlements of a single pile were derived from pile load tests (trial piles) taking into account the maximum working load of a single pile. For settlement calculations of the pile group the envelope area of all piles (in full diaphragm walls at Pier 6) in the foundation depth was taken as a basis. For this quasi-monolith the settlement calculations were performed as for a shallow foundation with a deep foundation level (e.g. according to DIN 4019). The total load was distributed over the total base of this quasi-monolith. The overburden stress in the foundation depth was then compared with the additional stress due to the bridge loads. The thickness of the compressible layer was limited to a depth (limit depth), where the additional stress reached 20% of the overburden stress.

Settlement calculations were performed with working loads without safety factors. Therefore, separate static calculations were carried out neglecting any safety factor in order to calculate working loads of each pile.

At Pier 6 (pylon axis) an average stress of 581 kN/m² was expected in the foundation depth. The additional stress of 39.6 kN/m² due to the dead load of concrete elements (piles, diaphragm wall, pile raft) had to be added, so that the total additional stress for settlement calculation amounted to 620 kN/m².

Depending on the modulus of compression for the marl and the limestone (beneath marl) the settlements of foundation were estimated to be:

$$s2 = 3.0 \text{ cm to } 4.0 \text{ cm} \quad (5)$$

with a limit depth of 70.3 m. With an estimated settlement of the single pile of:

$$s_1 = 0.5 \text{ cm} \quad (6)$$

the total settlements for final stage amounted to:

$$s_{total} = s_1 + s_2 = 3.5 \text{ cm to } 4.5 \text{ cm} \quad (7)$$

Differential settlements of the pier foundation due to load distribution within the pile group could be derived from settlement calculations of the box-shaped foundation and were estimated to $\Delta s \leq 0.5$ cm.

Regarding the rotation of the pier foundation several calculations were performed in order to consider load distribution, inclined rock surfaces in longitudinal and transversal directions and varying soil/rock modulus. Due to the results it was recommended to set a rotation of 1‰ for the pier foundation in the static model.

The settlement calculations for the final stage (see Table 11a) showed that the settlements of Pier 1 were less than the settlements of the other piers, because of lower load from superstructure at this pier. The same

**Table 11a:** Predicted and allowable settlements at final stage.

| **Pier** | **Predicted settlements at final stage** $s_{total} = s_1 + s_2$ |
|---|---|
| Pier 1 | 1,5 – 2,5 cm |
| Pier 2 | 4,0 – 5,0 cm |
| Pier 3 | 3,5 – 4,5 cm |
| Pier 4 | 2,5 – 3,5 cm |
| Pier 5 | 2,0 – 3,0 cm |
| Pier 6 | 3,5 – 4,5 cm |
| Pier 7 | 0,0 – 1,0 cm |
| Pier 8 | 0,0 – 1,0 cm |

situation occurs at Pier 5: due to the cables a part of the load from superstructure is transferred to Pier 6, which results in a minor foundation load at Pier 5.
Piers 1 to 6 are founded within marl. However, at Pier 6 the settlements are relatively low, although the total load is high in comparison to the other piers. The reason is that at Pier 6 the limestone (rock) is only a few meters below foundation level. The limestone was considered only at Pier 6 in the settlement calculations, because the interface was explored only in exploratory drillings at Pier 6.

However, the differential settlements for the superstructure shown in Table 11b are not relevant, because construction stages and settlements, which have already occurred until bearings for superstructure were installed, were not considered. Therefore, additional settlement calculations for the following construction stages were performed:

- Construction stage A: Start of construction works.
- Construction stage B: Completion of pier construction.
- Construction stage C: Launching of superstructure finished.
- Final stage.

**Table 11b:** Differential settlements after pier construction.

| **Pier** | **Differential settlements after pier construction** | |
|---|---|---|
| | $\Delta s_{predicted}$ | $\Delta s_{allowable}$ (superstructure) |
| Pier 1 | 2,0 – 2,5 cm | 2,7 cm |
| Pier 2 | 0,5 – 1,0 cm | 2,1 cm |
| Pier 3 | 0,5 – 1,0 cm | 2,4 cm |
| Pier 4 | 1,0 – 1,5 cm | 2,4 cm |
| Pier 5 | 2,0 – 2,5 cm | 5,4 cm |
| Pier 6 | 3,0 – 3,5 cm | 7,1 cm |
| Pier 7 | 0,0 – 0,5 cm | 1,2 cm |
| Pier 8 | | |


**Figure 27.** Main construction sequences of deep foundation works for box-shaped foundation at Pier 6 on man-made working platform at Ada Ciganlija Island (construction of diaphragm walls and piles, removal of pile heads after concreting, placing of blinding layer, reinforcement works, construction of pile raft, scaffolding and formwork for pylon).

Only settlements and in particular differential settlements, which occur after construction stage C, influence the superstructure, because bridge bearings were installed just before this construction stage. However, these calculations have shown that the assumptions for the static model of superstructure are on the safe side and that the expected differential settlements are lower than those considered in the static calculation of the superstructure. To date settlement measurements indicate that real settlements will not exceed the predicted settlements.

### *3.7 Foundation construction works*

Foundation works started in the summer of 2008. The deep foundation works for all piers and auxiliary foundations for launching were finished within the defined time schedule.

Construction for the foundation and the pylon of Pier 6 took place on a man-made peninsula at Ada Ciganlija Island (see Figure 27), which was filled prior to the bridge construction. The exceptional challenge for the foundation works was the access situation, which had to be accomplished with barges, ferries and boats since Ada Ciganlija Island was dedicated an environmental protection and recreation area of the City of Belgrade.

Consequently, all the earth and foundation works and in particular the concreting phases for the diaphragm wall, the piles and the pile raft had to be planned carefully in advance since concrete had to be delivered just in time. In peak periods up to 400 m³ per hour of concrete were required, which were transported with barges to the man-made construction platform. Three modern crawler type carrier machines (one Liebherr HS875 and two HS855) and a powerful large diameter drilling machine (Bauer BG 40) were used in parallel in order to complete the entire deep foundation works at Pier 6 within 12 weeks only (Hinterplattner et al. 2011). The entire bridge construction works were finished in autumn 2011 and the grand opening of the bridge was on New Year's Eve 2011, thus, the bridge has been in operation since the beginning of 2012.

**Figure 28.** Sava Bridge building construction in progress (January 2011) and visualisation of the completed bridge, the new spectacular landmark of Belgrade.

## 4 COMPARISON OF THREE DIFFERENT FOUNDATION CONCEPTS

Finally, the three different foundation concepts presented are compared and discussed.

Ground improvement facilitates, primarily, a homogenization of ground conditions, an increase of the bearing capacity and in many cases an acceleration of consolidation settlements but it is not the primary target to reduce settlements to a minimum. Hybrid foundations are a combination of ground improvement during the installation works and deep foundation behaviour after completion by one and the same technique, thus, providing both better ground conditions and transfer of (high) loads at depth in the ground. Deep foundation either bridges unfavourable ground layers to good bearing soil or rock layers or transfers (very high) loads at depth in the ground, thus, avoiding major settlements.

In the following figures the concepts are illustrated and it is demonstrated that each of the concepts may be justified depending upon the ground conditions, structural and serviceability requirements of the buildings, and economical factors (time and cost). Depending on the ground conditions and the function with respect to bearing behaviour and deformation behaviour (serviceability) each concept exhibits advantages and benefits.

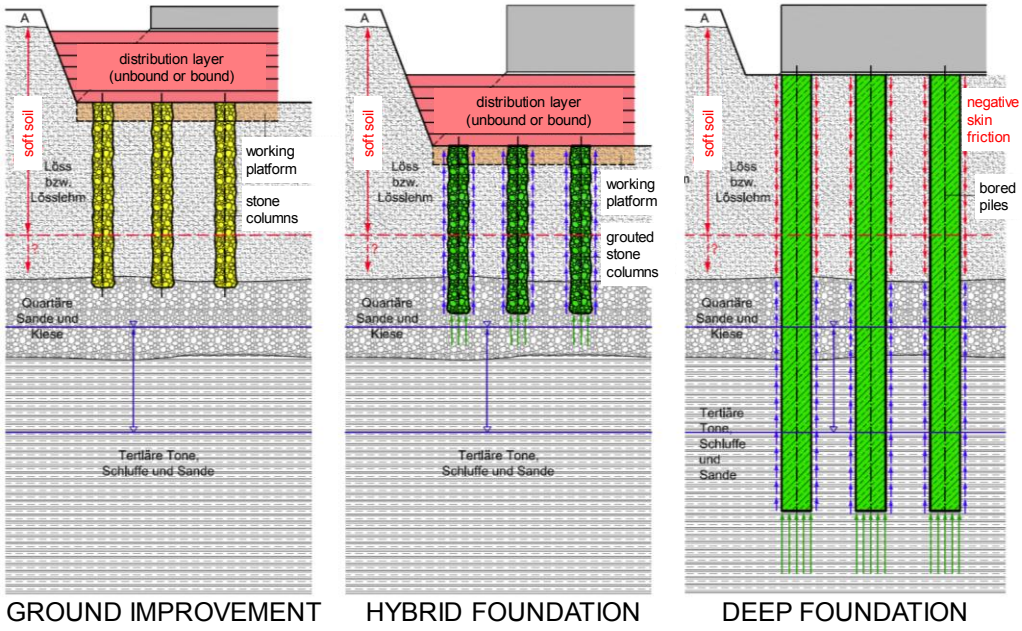


**Figure 29.** Comparison of foundation concepts.

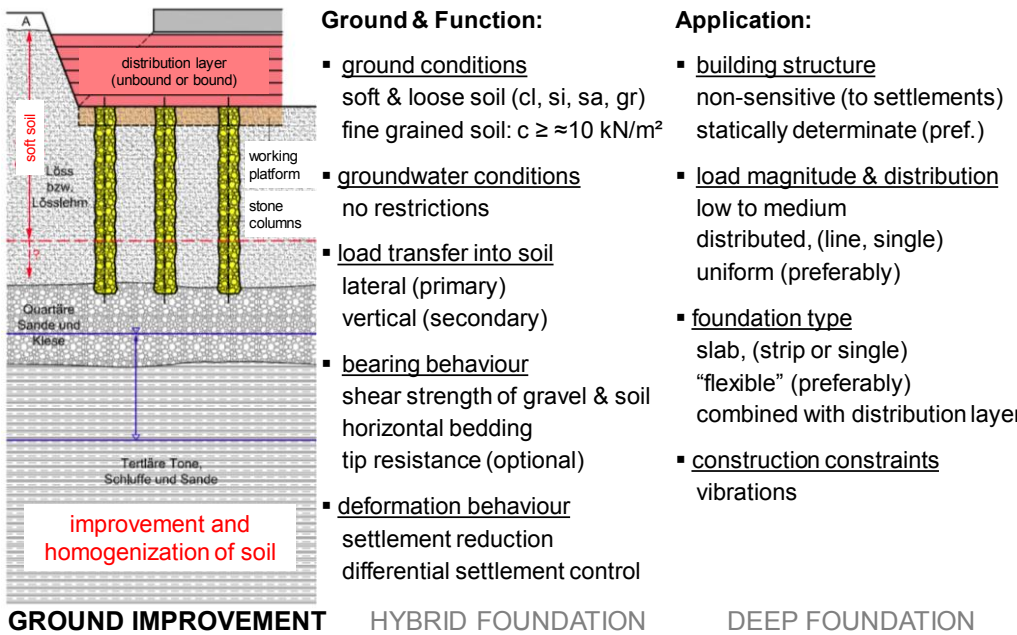


**Figure 30.** Ground improvement.

**Ground & Function:**

- ground conditions
  soft & loose soil (cl, si, sa, gr)
  collapsible soil (!)
- groundwater conditions
  no restrictions
- load transfer into soil
  lateral (after installation)
  vertical (after hydration)
- bearing behaviour
  material compressive strength
  skin friction (improved soil)
  tip resistance (optional)
- deformation behaviour
  medium to low settlements
  low differential settlements

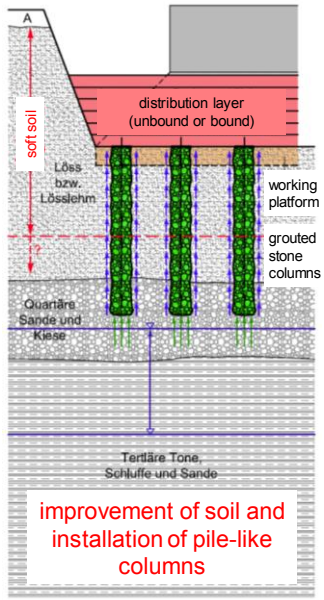


**Application:**

- building structure
  sensitive (to settlements)
  statically (in)determinate
- load magnitude & distribution
  medium to high
  single, line & distributed
  uniform to irregular
- foundation type
  slab, strip or single
  "flexible" or "rigid"
  combined with distribution layer
- construction constraints
  vibrations

GROUND IMPROVEMENT **HYBRID FOUNDATION** DEEP FOUNDATION

**Figure 31.** Hybrid foundation.

**Ground & Function:**

- ground conditions
  soil & rock (any)
- groundwater conditions
  no restrictions (pile install.)
- load transfer into soil
  vertical (horizontal, bending)
  (floating piles – end bearing p.)
- bearing behaviour
  pile compressive strength
  skin friction (floating)
  tip resistance (end bearing)
- deformation behaviour
  settlement minimization
  differential settlement
  minimization

**Application:**

- building structure
  very sensitive (to settlements)
  statically indeterminate (pref.)
- load magnitude & distribution
  high to very high
  single, line & distributed
  uniform to irregular
- foundation type
  slab, strip or single (any)
  capping beams etc.
  highly reinforced
  "rigid"
- construction constraints
  depending on pile type and
  piling system

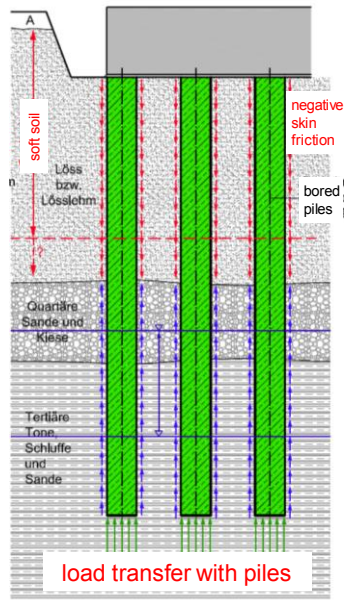


GROUND IMPROVEMENT HYBRID FOUNDATION **DEEP FOUNDATION**

**Figure 32.** Deep foundation.

## 5 CONCLUSIONS

At first the ground improvement concept and in particular the settlement behaviour of the new stadium in Klagenfurt is presented which was built from 2006 to 2007 for the European Soccer Championship EURO 2008. Due to the unfavourable soil conditions consisting of unconsolidated lake deposits underlain by moraine and the bed rock in varying depth, large settlements were predicted and significant differential settlements were expected due to non-uniform loads which had to be taken into account for compatibility requirements between adjacent structural elements. Ground conditions were improved and homogenized to depths of 18 m by installing stone columns using the vibro replacement technique. Long-term monitoring of settlements and a well instrumented field trial have been carried out to document the time-dependent settlement process and to investigate the performance of the floating stone column foundation. Back analysis using the Soft Soil Creep (SSC) model was performed to calculate the settlement process and final settlements. Results match well with measurements from extensometers and are in accordance with measured settlements of the foundation slab at the west side. Agreement on the east side is less satisfactory; one possible reason for this could be that the load has been overestimated in this part of the foundation.

Secondly the innovative hybrid foundation concept of CCPP Malženice is presented. The foundation measures for the 400 MW gas fired combined cycle power plant at Malženice, in the western part of Slovakia was constructed by E.ON Elektrárne, s.r.o., the Trakovice based subsidiary of E.ON Kraftwerke GmbH of Hannover, Germany. The foundations comprise deep soil improvement and deep foundation elements (hybrid foundation), and soil stabilization. The hybrid foundation was realized by grouted stone columns (pile-like bearing elements) through the collapsible loess layer and embedded in the gravel layer complex. The columns were produced by the deep vibro replacement technique and deep improvement of the soil around the columns due to the vibration process. Thus, anticipation of collapse of the soil structure and compaction of loess was caused. The working platform, stabilized by the mixed-in-place method with a lime-cement binder (KZM), ensured the deep improvement and deep compaction. The filling above the columns up to the level of the blinding layer has also been stabilized with KZM. The presented innovative hybrid foundation concept was supervised by an extensive quality assurance system and was executed alternatively to the original foundation concept, which was based on bored piles. Thus, significantly shorter deep foundation elements in comparison with piles according to the original foundation concept could be realized due to avoiding negative skin friction along the deep foundation elements.

Finally, the deep foundation concept of the new cable-stayed bridge over the Sava River in Belgrade near the entry of the Sava River into the River Danube has been presented. The foundation at 8 piers for the new bridge over the Sava River in Belgrade was successfully accomplished based on an innovative design procedure according to EC 7. The Sava Bridge was the first project of that dimension which was executed in accordance with EC 7 using the national application rules of Austria for pile foundations of a major bridge. In conclusion the foundations were economically designed in such a way that they exhibit sufficient overall safety against failure and also satisfactory behaviour in the serviceability limit-state, thus, considering the life time of the bridge.

All the bridge foundations showed satisfactory settlement behaviour already during construction and after completion. The bridge is the new landmark of Belgrade; nevertheless the deep foundations are invisible but will provide a safe basis for the lifetime of the new Sava Bridge.

When comparing the different foundation concepts, in conclusion, no ranking can be made with respect to the issue of which is the best concept. Each may be justified depending upon the ground conditions, structural and serviceability requirements of the buildings, and economic factors (time and cost). Since every single building is a prototype taking into account the ground conditions and the function with respect to bearing behaviour and deformation behaviour (serviceability) the most appropriate foundation concept has to be assessed in a profound geotechnical design procedure based on a comprehensive ground exploration and soil investigation programme, which needs continuous verification not only in the design phase but also during execution (monitoring etc.).

## REFERENCES


Adam D. & Geotechnik Adam ZT GmbH. 2008a. Geotechnical Report for the Construction of a 400 MW Combined Cycle Power Plant (CCPP) in SK 91929 Malzenice, Slovakia (in German): A-2345 Brunn am Gebirge, Wiener Straße 66-72/15/4; (unpublished).

Adam D. & Geotechnik Adam ZT GmbH. 2008b. Quality control plan for the foundation works (in German). A-2345 Brunn am Gebirge, Wiener Straße 66-72/15/4; (unpublished).

Adam, D. & Geotechnik Adam ZT GmbH. 2008c. Wörtherseee-Stadion Klagenfurt, Gründungsarbeiten, Geotechnischer Schlussbericht. A-2345 Brunn am Gebirge, Austria.

Adam, D. & Markiewicz, R. 2011. A new spectacular bridge over the Sava River in Belgrade – foundation design and construction. In: *Proc. of 10th International Geotechnical Conference*, 176-195, Slovak University of Technology Bratislava, Faculty of Civil Engineering, Department of Geotechnics, 30 – 31 May 2011, Bratislava, Slovakia.

Adam, D., Schweiger, H.F., Markiewicz, R. & Knabe, T. 2010. EURO 2008 Stadium Klagenfurt – Prediction, Monitoring and Back Calculation of Settlement Behaviour. In: *Proc. of the XIVth Danube-European Conference on Geotechnical Engineering: From Research to Design in European Practice*, 217-230, Slovak University of Technology in Bratislava, 2 – 4 June 2010, Bratislava, Slovakia.

Adam, D., Turcek, P. & Paulmichl, I. 2009. Innovative hybrid ground improvement and deep foundation concept for the CCPP Malženice (Slovakia). In: *Proc. of 9th International Geotechnical Conference*, 59-68, Slovak University of Technology Bratislava, Faculty of Civil Engineering, Department of Geotechnics, 1 – 2 June 2009, Bratislava, Slovakia.

Bauer Spezialtiefbau GmbH 2009. *Belgrad Sava Bridge, Pfahlprobebelastung*, Bericht Nr. 04/02/09. February 2, 2009, unpubl.

Bautechnische Versuchs- und Forschungsanstalt Salzburg. 2006. Prüfbericht, Baugrunderkundung, Probefeld Stadion Klagenfurt. A-5020 Salzburg, Austria.

Bjerrum, L. 1967. Engineering geology of Norwegian normally-consolidated marine clays as related to settlements of buildings. Seventh Rankine Lecture. *Géotechnique* **17**, 81-118.

Brandl, H. 2003. Box-shaped foundations of bored and auger piles (or diaphragm walls). *Proceedings of the 4th International Geotechnical Seminar on Deep Foundations on Bored and Auger Piles*, 349-358, Millpress, Rotterdam.

Brandl, H. 2005. Settlement-Minimizing pile and diaphragm wall foundations for high rise buildings and bridges. *Geotechnics in urban areas*. Bratislava, June 27-28, 2005.

Brinkgreve, R.B.J., Broere, W. & Waterman, D. 2006. *Plaxis, Finite element code for soil and rock analyses*, user's manual. The Netherlands.

DIN 1054. 2005. Subsoil – Verification of the safety of earthworks and foundations.

Fross, M., Adam, D. & Hofmann, R. 2010. Pile Foundations for River Bridges according to EC 7-1. *Proc. of the XIVth Danube-European Conference on Geotechnical Engineering*, *From Research to Design in European Practice*, 144-166, Slovak University of Technology in Bratislava, 2 – 4 June 2010, Bratislava, Slovakia.

Gäb, M., Schweiger, H.F., Thurner, R. & Adam, D. 2007. Field trial to investigate the performance of a floating stone column foundation (in coop. with). In: *Proc. of XIV European Conference on Soil Mechanics and Geotechnical Engineering (XIV ECSMGE),* 1311-1316, Madrid, Spain. Millpress, Rotterdam.

Gäb, M., Schweiger, H.F., Kamrat-Pietraszwska, D. & Karstunen, M. 2008. Numerical analysis of a floating stone column foundation using different constitutive models. In Karstunen and Leoni, *Geotechnics of Soft Soils*, volume **1**, 137-142. Tylor & Francis Group, London.

Geotechnik Adam ZT GmbH 2009a. Geotechnical Interpretive Report for the Bridge over the River Sava – Trial Piles. February 26, 2009, (unpublished).

Geotechnik Adam ZT GmbH 2009b. Geotechnical Interpretive Report for the Bridge over the River Sava – Piers 1 to 7. Revision B. April 30, 2009, (unpublished).

Geotechnik Adam ZT GmbH 2009c. Settlement Report for the Bridge over the River Sava – Piers 1 to 8. July 29, 2009, (unpublished).

Hinterplattner, B., Markiewicz, R. & Adam, D. 2011. *Sava Bridge Belgrad – Eine innovative Pylonfundierung für eine spektakuläre Schrägseilbrücke*. 8. Österreichische Geotechniktagung 03.-04.02.2011, Wien.

http://www.eon-elektrarne.com/pages/ekw_en/index.htm

Ingenieurgemeinschaft Garber & Dalmatiner Zivilingenieure 2005a. Bodenmechanisches Gutachten zum Projekt Wörtherseee-Stadion Klagenfurt, Neubau. A-8010 Graz bzw. A-9500 Villach, Austria.

Ingenieurgemeinschaft Garber & Dalmatiner Zivilingenieure 2005b. Ergänzung zum bodenmechanischen Gutachten zum Projekt Sportpark Wörthersee, Stadion EURO 2008, Klagenfurt. A-8010 Graz bzw. A-9500 Villach, Austria.

Janbu, N. 1967. The resistant concept applied to soils, *Géotechnique* **17**: 81-118.

ÖNORM B 1997-1-1. 2007. Geotechnical design, General rules – National specifications concerning ÖNORM EN 1997-1 and national supplements.

ÖNORM B 1997-1-3. 2007. draft version: Berechnung und Bemessung in der Geotechnik – Pfahlgründungen, Ermittlung der Tragfähigkeit (in German).

ÖNORM B 4440. 2001. Erd- und Grundbau, Großbohrpfähle, Tragfähigkeit (in German).

ÖNORM B 4431-2. 1986. Geotechnical engineering; permissible soil pressures; settlement observations.

ÖNORM EN 1997-1 (EC 7) 2006. Geotechnical design, General rules.

Steinkühler, M. et al. 2010. *Ein neues Wahrzeichenzeichen für Belgrad: Schrägseilbrücke mit 200 m Pylon über die Sava in Belgrad, Serbien*. Betontag 22.-23.04.2010, ÖVBB, Wien.

Vermeer P. & Neher, H. 2000. A soft soil model which accounts for creep. *Beyond 2000 in Computational Geomechanics - 10 years of PLAXIS International*, 249-262, Balkema, Rotterdam.